

**Inhibiting Epidermal Growth Factor Receptor Signalling Potentiates Mesenchymal-
Epithelial Transition of Breast Cancer Stem Cells and their Responsiveness to
Anticancer Drugs**

Kanakaraju Manupati^{1,2}, Neha R Dhoke^{1,2}, Tanusree Debnath³, Ragini Yeeravalli^{1,2}, Kalpana
Guguloth¹, Shahrzad Saeidpour¹, Utpal Chandra De⁴, Sudhan Debnath³, Amitava Das^{1,2*}

¹Centre for Chemical Biology, CSIR-Indian Institute of Chemical Technology, Uppal Road,
Hyderabad – 500 007, India

²Academy of Scientific & Innovative Research, 2 Rafi Marg, New Delhi – 110 001, India

³Department of Chemistry, Maharaja Bir Bikram College, Agartala – 799 004, Tripura, India

⁴Department of Chemistry, Tripura University, Agartala–799 130, Tripura, India

*Corresponding Author: Dr. Amitava Das, *PhD*, Ph No.: +91-40-27191873; E-mail:
amitavadas@iict.res.in; amitavadas.iict@gov.in

Running Title: EGFR inhibitor sensitize breast CSC to chemotherapeutic drug

Article type : Original Articles

Conflict of Interest: “The authors declare no potential conflicts of interest.”

This article has been accepted for publication and undergone full peer review but has not
been through the copyediting, typesetting, pagination and proofreading process, which may
lead to differences between this version and the Version of Record. Please cite this article as
doi: 10.1111/febs.14084

This article is protected by copyright. All rights reserved.

Key words: CD24⁻/CD44⁺-breast CSCs, mammospheres, EGFR, MET, chemoresponsiveness.

Abbreviations: EGFR- Epidermal growth factor receptor, TNBC- Triple negative breast cancer, EMT- Epithelial to Mesenchymal transition, RTK- Receptor tyrosine kinase, ER- Estrogen receptor, PR-progesterone receptor, Her2- Human epidermal growth factor receptor2, CSCs- Cancer Stem Cells, MET- Mesenchymal to Epithelial transition, CD- Cluster of differentiation.

Abstract

Recurrence of breast cancer in patients is a persisting challenge to medical fraternity. Breast tumor contains a small population with high tumor initiating and metastatic potential known as Cancer Stem Cells (CSCs) that are resistant to existing chemotherapeutics. CSCs contribute to the aggressiveness of Triple Negative Breast Cancers (TNBCs) thereby necessitates identifying molecular targets on breast CSCs. TNBC cell line *MDA-MB-231*, as compared to *MCF-7* depicted a higher expression of Epidermal Growth Factor Receptor (EGFR). Thus naturally occurring flavanone, chrysin with limited potential as chemotherapeutic agent was structurally modified by designing analog with EGFR binding affinity using molecular docking approach and synthesised. Chrysin analog, CHM-09 and known EGFR inhibitors depicted a comparable anti-proliferative, anti-migratory activity along with induction of apoptosis and cell cycle arrests in *MDA-MB-231*. Furthermore, sorted CD24⁻/CD44⁺-breast CSCs and CD24⁺-breast cancer cells from *MDA-MB-231* depicted markedly high expression of EGFR in the former than latter. CHM-09 and EGFR inhibitors could perturb EGF-induced EGFR signalling of breast CSC's proliferation, migration,

mammosphere formation and mesenchymal tri-lineage differentiation. CHM-09 or EGFR inhibitors not only led to inactivation of EGFR downstream signalling pathways like AKT, ERK and STAT3 but also induction of mesenchymal-epithelial transition as confirmed by decreased N-cadherin and increased E-cadherin expressions. Finally, combinatorial treatment of EGFR inhibitors and doxorubicin led to significant increase in breast CSCs responsiveness to chemotherapeutic drug. This study suggests that EGFR as a therapeutic target in breast CSCs and abrogation of EGFR signalling along with chemotherapeutic drugs as an effective approach against breast cancer.

Introduction

Cancer is an imbalance between cell-division and death that favours unlimited growth of tumor. Various tissue-specific cancers such as breast, lung, and liver, occur due to DNA mutations caused by physical or chemical mutagens. Among these, breast cancer is the second most common cause of morbidity and mortality in women [1]. To date, several anti-cancer therapeutics are targeted against a number of receptor tyrosine kinases (RTK) that are known to play major role in tumorigenesis by activating downstream signalling [2]. Among the RTKs, Transforming Growth Factor Receptor-beta has been reported to promote breast cancer metastasis through induction of epithelial-to-mesenchymal transition (EMT) [3], Vascular Endothelial Growth Factor Receptor as a mediator of breast tumor angiogenesis [4] and Platelet-derived Growth Factor Receptor as a predominant signalling pathway in maintenance of mesenchymal phenotype of breast cancer [5]. Literature suggests a crucial role of Epidermal Growth Factor Receptor (EGFR) in breast cancer cell proliferation and migration [6]. EGFR belongs to the ErbB tyrosine kinase family that comprises of four receptors such as EGFR/ErbB1, HER2/ErbB2, HER3/ErbB3 and HER4/ErbB4 [7]. Among these, EGFRs are highly expressed in human malignant tumors [8] but is a poor prognostic

factor in breast cancer [9]. The activation of EGFR phosphorylates its downstream signalling molecules AKT, STAT3 that are involved in cellular migration and MAPK signalling which is implicated in cell proliferation [10]. While breast cancer patients treated with EGFR inhibitors such as erlotinib and gefitinib have been shown with minimum clinical activity [11] but with reduced side-effects in comparison to conventional chemotherapeutic drugs [12]. Therefore, it is pertinent to target EGFR signalling with more potent inhibitors which are naturally derived chemicals as cancer therapeutics.

Chrysin, a flavonoid is a natural phytochemical abundantly found in many plant extracts. It shows cytotoxicity against colon, lung, cervical, liver, prostate, and pancreatic cancer [13]. The use of chrysin as a chemotherapeutic agent has limitations such as poor therapeutic potential and poor absorption, rapid metabolism, and fast systemic elimination [14]. Although liposomal nanoparticles conjugated with chrysin have been used for efficient anticancer drug delivery [15], we hypothesize that designing of synthetic analogs of chrysin against a specific molecular target may improve its efficacy as chemotherapeutic agents.

In spite of available chemotherapeutic agents against breast cancer, reoccurrence of cancer often arises due to the presence of a small sub-population of cancer cells known as Cancer Stem Cells (CSCs). CSCs are tumor-initiating cells with self-renewal ability and high metastatic potential [16]. CSCs are resistant to existing chemotherapy and radiotherapy due to higher expression of efflux transporters, enhanced DNA repair mechanism and resistance to apoptosis [17].

In the present study, a higher expression of EGFR was observed in aggressive triple negative breast cancer (TNBC) cell line, *MDA-MB-231* as compared with luminal breast cancer cell line, *MCF-7*. This led us to design and synthesize a chrysin analog, CHM-09 that binds to EGFRs confirmed by molecular docking studies and cellular thermal shift assays. Inhibition

of EGFR signalling pathway by known EGFR inhibitors or CHM-09 caused significant perturbation on proliferation and migration of parental *MDA-MB-231* cells as well as sorted breast cancer cells (CD24⁺) and breast CSCs (CD24⁻/CD44⁺) populations. This was followed by an interesting observation of a higher expression of EGFR in the breast CSCs as compared to breast cancer cells. Both CHM-09 as well as EGFR inhibitors could inhibit the EGF-induced increased proliferation, migration, mammosphere formation and tri-lineage differentiation (owing to mesenchymal phenotype) of CD24⁻/CD44⁺-breast CSCs along with concomitant increase in epithelial and decrease in mesenchymal gene and protein expression. A simultaneous treatment with chemotherapeutic drugs and CHM-09 or EGFR inhibitor in breast CSCs made them increasingly responsive to the anticancer drugs. This study emphasises the role of EGFR as a therapeutic target for breast CSCs and a combination therapy of EGFR inhibitors and chemotherapeutic agents as a potential strategy targeting breast CSCs to prevent cancer recurrence.

Results

Differential expression of EGFR in breast cancer cell lines: EGFR expression in *MCF-7* (ER⁺/PR⁺/Her2⁻, Luminal type) and *MDA-MB-231* (ER⁻/PR⁻/Her2⁻, Basal type) breast cancer cells using semi-quantitative RT-PCR (Fig 1A) and immunoblotting (Fig 1B) depicted relatively high level in *MDA-MB-231* as compared to *MCF-7*. This observation suggests a crucial role of EGFR in the aggressive triple negative breast cancer (TNBC) types which is associated with poor prognosis and reduced survival in patients [18].

Molecular docking of chrysin analogs on EGFR: Chrysin (Fig 1C), a naturally occurring flavanone having a limited clinical potential as an anticancer agent led us to design using chemical docking approach and synthesize its analog, CHM-09 (Fig 1D) with improved

binding affinity to EGFR (Fig 1E). The low resolution X-ray crystal structures of different EGFR (PDB ID: 3W32, 3W33, 3POZ and 3W2R) complexed with co-ligands have been retrieved from RCSB protein data bank (www.rcsb.org). The final selection of EGFR was performed on the basis of the docking accuracy by calculating root mean square deviation (RMSD). The RMSD values were calculated by superimposing best docked poses of co-ligands on its native co-ligand. The RMSD value has been observed to be the lowest for 3W32 (0.8254) (Table 1). The XP glide scores of co-ligands with receptors 3W32, 3W33 were -14.297 and -12.624, respectively and the important interacting amino acid residues were observed to be MET-793, PHE-856, LEU-718 (Fig 1F). The interacting amino acid residues for CHM-09 were observed to be MET-793, ASP-855 (2), LYS-745 with XP glide score of -12.187 (Fig 1E, 1F). Similarly, molecular docking of commercially available EGFR inhibitors AG-1478 and PD-153035 depicted that ASP-855 is the crucial amino acid residue for inhibition which is also present in case of CHM-09 (data not shown). Other than the common interactions with EGFR inhibitors, CHM-09 also have interactions with MET-793, LYS-745. Based on the active site amino acid residues and XP glide score of both CHM-09 and co-ligands (Fig 1G, 1H), chrysin was isolated from the bark of *Oroxylum indicum* (Fig 2A), and chrysin analog, CHM-09 was synthesized as described in the scheme (Fig 2B) and characterized using spectral analysis (Fig 2C, 2D) before subjecting for further evaluations. To further support the *in silico* molecular docking of EGFR-CHM-09 interaction, we performed cellular thermal shift assay (CETSA) to elucidate the binding of CHM-09 to EGFR in *MDA-MB-231* cells. CETSA evaluates the binding of a ligand or small molecule to its target protein that leads to increased target protein stabilization at differential temperature [19]. For binding assessment, cells were treated with EGF (25ng/mL), CHM-09 and EGFR inhibitors-AG1478 and PD153035 (25 μ M) for 1h followed by immunoblotting. Optimum EGFR stabilization by CHM-09 binding was observed till 46°C (Fig 3A). Cells

treated with CHM-09, PD153035 depicted EGFR expression at 50°C as compared to unbound protein in DMSO-treated cells that depicted a complete disappearance of EGFR at the same temperature (Fig 3A). The significant shift in melting temperatures of EGFR and its stabilization upon addition of the CHM-09 indicated that both the compounds bind to this protein.

Proliferation of breast cancer cells by EGFR inhibitors: Next, we evaluated the anti-proliferative potential of our synthesized chrysin analog, CHM-09 and compared it with its parent molecule, chrysin and EGFR inhibitors, AG1478 and PD153035 using cell viability assays. The compound CHM-09 depicted a higher efficacy against a panel of TNBC cell lines, *MDA-MB-231* (Fig 3B), *MDA-MB-453* (Fig 3C), *MDA-MB-468* (Fig 3D) and *BT-549* (Fig 3E) with low IC_{50} values (μM) 4.52 ± 1.4 , 8.35 ± 0.24 , 7.88 ± 0.2 and 10.17 ± 0.8 , respectively as compared to *MCF-7* (Fig 3F; IC_{50} (μM): 25.71 ± 0.1). The anti-proliferative potential of chrysin against both the cell types luminal and TNBCs was relatively comparable (IC_{50} (μM): *MCF-7* - 32.08 ± 2.1 and *MDA-MB-231* - 40.01 ± 6.7 , *MDA-MB-468* - 36.02 ± 1.2 , *MDA-MB-453* - 28.96 ± 1.82 and *BT-549* - 33.97 ± 2.4). EGFR inhibitors, AG1478 depicted an equal anti-proliferative effect in *MCF-7* (IC_{50} : $11.47 \pm 1.2 \mu M$) and *MDA-MB-231* (IC_{50} : $11.72 \pm 0.2 \mu M$) cells. In contrast, PD153035 another EGFR-specific inhibitor reduced proliferation of *MDA-MB-231* cells by half of inhibitor concentration (IC_{50} : $3.20 \pm 0.5 \mu M$) as compared to *MCF-7* (IC_{50} : $6.69 \pm 0.9 \mu M$). However, TNBC cell lines depicted relatively high proliferation in presence of PD153035, with IC_{50} values (*MDA-MB-468* - $15.4 \pm 0.8 \mu M$, *MDA-MB-453* - $10.53 \pm 0.92 \mu M$ and *BT-549* - $26.1 \pm 1.3 \mu M$). Interestingly, CHM-09 depicted a less toxicity towards *HEK293*, human primary kidney control cells with 5-10 -fold high IC_{50} values ($53.04 \pm 0.72 \mu M$) as compared to TNBCs (Fig 3G) suggesting a good therapeutic window. EGFR inhibitors depicted relatively similar toxicity towards *HEK293* control cells

(AG1478-22.15±3.09µM, PD153035-18.40±0.13µM) (Fig 3G). These results correlated well with EGFR expression levels in these breast cancer cell lines indicating that chrysin analog, CHM-09 with improved EGFR binding ability effectively decreases the cell viability in TNBC cell lines that expresses relatively high EGFR.

Modulation of aggressive TNBC cell cycle and apoptosis by EGFR inhibitors: To further substantiate the *in vitro* anti-proliferative effect of EGFR inhibitors and/or chrysin analog, CHM-09 at low micromolar range on *MDA-MB-231* cells, we evaluated the BrdU incorporation using cell cycle analysis. CHM-09 treated cells depicted 62.3% of cells in G₀/G₁ phase of the cell cycle as compared to 53.3% in vehicle control group (Fig 4A) indicating a G₀/G₁ cell cycle arrest. EGFR inhibitors, AG1478 and PD153035 treatment also resulted in G₀/G₁ cell cycle arrest with 62.4% and 64.5%, respectively. The expression of unique cyclins and cyclin-dependent kinases (CDKs) along with CDK inhibitors (CKIs) occur during the cell cycle progression. The gene expression levels of cyclin D, cyclin E and their CDK partners, CDK2 that regulates G₀/G₁ phase was markedly decreased in cells treated with inhibitors as well as CHM-09 as compared with vehicle control (Fig 4B).

To further corroborate the cell cycle gene expression of EGFR inhibitors and/or chrysin analog, CHM-09 on *MDA-MB-231* cells, we evaluated the protein expression levels too. Expression of CDK4 and CDK2 and their partners Cyclin D and Cyclin E regulates G₁ phase of cell cycle was markedly decreased in cells treated with inhibitors indicates that accumulation of cells at G₀/G₁ phase (Fig 4C). These results correlated well with BrdU cell cycle analysis data. In contrast, cyclin B regulates G₂/M phase of cell cycle was increased whereas with CDK1 no obvious changes was observed in presence of inhibitors as compared to vehicle control indicates M phase progression. This observation was further substantiated

by a concomitant increased expression of CKI, p21 and decreased expression of p27 in presence of inhibitors (Fig 4C) suggesting that major role of p21 in preventing the CDK4 and CDK2 complexes and their interacting partners thereby arresting cells at the G₀/G₁ phase of cell cycle. These results collectively suggests an apoptotic cell death by these treatments, led us to evaluate apoptotic populations using flow cytometric analysis. A significantly high percent (~98.4%) of cells were observed to undergo apoptosis in CHM-09 treated cells as compared to vehicle control (Fig 5A). Similarly, the EGFR inhibitors AG1478 and PD153035 induced apoptosis with 84.4% and 94.5%, respectively (Fig 5A). Further substantiating this observation, pro-apoptotic genes –Bax and Bid (Fig 5B) as well as proteins–BAX, Caspase3 and Annexin V (Fig 5C) expression levels were significantly high in cells treated with either CHM-09 or EGFR inhibitors with a concomitant decrease in anti-apoptotic, Bcl-2 expression at gene (Fig 5B) and protein level (Fig 5C). Also a significant increase in expression of p53 further substantiated induction of apoptotic signalling.

Attenuation of EGFR downstream signalling in aggressive TNBC cells by CHM-09: EGFR activation has been associated with multiple biological processes in cancer progression such as cell proliferation, migration and metastasis through different signalling pathways [20]. To evaluate the effect of CHM-09 on signal transduction mechanism, we performed immunoblot analysis of EGFR downstream signalling pathways-AKT, ERK and STAT3. Aggressive TNBC, *MDA-MB-231* cells that express high EGFR were treated with increasing concentration of CHM-09 depicted a dose-dependent decrease in phosphorylation of EGFR, AKT, ERK and STAT3 (Fig 6A). Similar CHM-09-mediated dose-dependent decrease in phosphorylation of these signalling mediators was also observed in *BT-549* (Fig 6B), *MDA-MB-453* (Fig 6C) and *MDA-MB-468* (Fig 6D). β -catenin, a downstream target of AKT signalling pathway [21], was also downregulated in CHM-09 treated cells indicating that

AKT attenuation leads to downregulation (decrease in phosphorylation) of β -catenin. Inhibition of EGFR by PD153035 also abolished activation of AKT, STAT3 and ERK signalling pathways responsible for cell migration and proliferation, respectively (Fig 7A). In order to confirm if this observation holds true, we performed proliferation assay in *MDA-MB-231* cells treated with EGF in presence/absence of EGFR, ERK, AKT and STAT3 signalling blockers at indicated doses. The EGF-induced proliferation was significantly decreased by CHM-09 similar to EGFR inhibitors, AG1478 and PD153035 (Fig 7B). Also wortmannin, PD98059 and static inhibitors of AKT, ERK and STAT3, respectively could significantly decrease EGF-induced proliferation (Fig 7B). Furthermore, addition of CHM-09 along with EGFR inhibitors or AKT and ERK inhibitors did not alter the cellular proliferation as compared with when added separately (Fig 7B). However, combination of CHM-09 and static significantly reduced proliferation as compared to static alone (Fig 7B) suggesting unique EGFR-STAT3 signalling pathway to regulate cell proliferation of these aggressive TNBCs. Next, we analyzed EGF-induced migration potential of *MDA-MB-231* cells in presence/absence of pathway inhibitors by scratch/migration assay. The rate of cell migration was evaluated temporally at 6, 12 and 24h time-points. EGF-induced migration was significantly attenuated by these inhibitors at treated concentrations (Fig 7C). Combinations of CHM-09 with these pathway inhibitors depicted a further significant decrease in cell migration by wortmannin and static (Fig 7C) suggesting a role of EGFR-AKT and EGFR-STAT3 signalling-mediated regulation of cell migration in aggressive TNBCs (Fig 7C). Aggressive property of TNBCs are contributed by a small highly migratory population known as Breast Cancer Stem Cells (CSCs) that differentially express specific cluster of differentiation (CD) markers on their cell surface [22,23].

High EGFR expression in breast CSCs renders them sensitive to EGFR inhibitors: Breast CSCs were sorted separately from a panel of TNBC cell lines – *MDA-MB-231*, *MDA-MB-453*, *BT-549* and *MDA-MB-468* based on presence or absence of CD24 cell surface marker (Fig 8A). Subsequently CD24⁻ cell populations were further subjected to CD44 selection (Fig 8A). The sorted CD24⁻/CD44⁺ (breast CSCs – percent yield of total: 9.3±1.6) cells expressed CD44 and were negative for CD24 whereas CD24⁺ (breast cancer cells – percent yield of total: 42.9±6.1) were positive for CD24 cell surface markers as analyzed using confocal imaging (Fig 8B). Additionally, flow cytometry analysis revealed 77.5% CD44 expressing cells while negative for CD24 surface marker expression thereby confirming the purity of these CD24⁻/CD44⁺ sorted fractions (Fig 8C). Upon characterization, CD24⁻/CD44⁺ depicted a marked increase in CSC-specific genes expression -ALDH1, MUC1, ABCG2, CD133 (Fig 8D) as compared to CD24⁺ sorted populations. CD24 gene expression was lacking in CD24⁻/CD44⁺ population (Fig 8D). ALDH1, an enzyme which is expressed at high levels in CSCs is known to be major characteristic feature of breast CSCs. Our sorted populations, CD24⁻/CD44⁺ exhibited a 100% aldefluor fluorescence as compared to control (DEAB) indicating an ALDH⁺ population (Fig 8E). Encouragingly, a markedly high level of EGFR expression was observed in CD24⁻/CD44⁺ as compared with CD24⁺ sorted cell populations (Fig S1). Next, cell viability of the sorted CD24⁻/CD44⁺-breast CSC populations from TNBC cell lines depicted a markedly decrease in cell proliferation in presence of CHM-09 with low IC₅₀ values (μM) of 1.34±0.37 (*MDA-MB-231*), 6.1±0.3 (*MDA-MB-453*), 4.3±0.3 (*BT-549*) and 3.2±0.1 (*MDA-MB-468*) (Fig 9A) as compared with CD24⁺ populations (IC₅₀ values (μM) of 8.8±2.17 (*MDA-MB-231*), 17.6±1.1 (*MDA-MB-453*), 18.9±1.2 (*BT-549*) and 14.9±1.2 (*MDA-MB-468*) (Fig 9B). The effect of CHM-09 on breast CSCs was 1.7-4.0 –fold higher than EGFR inhibitor, PD153035 (Fig 9A). This observation suggests a higher expression of

EGFR in breast CSCs as compared with breast cancer cells leads to better inhibition of EGFR by these inhibitors thereby modulating further downstream signalling-mediated cell viability.

Attenuation of EGFR downstream signalling in breast CSCs: To further support the observation of EGFR inhibition led to decrease in physiological phenotype of breast CSCs we explored the downstream signalling of EGFR in presence of CHM-09 as well as various receptor blockers using immunoblotting techniques. An EGF-induced increased phosphorylation of EGFR as well as its downstream kinases –ERK, AKT and STAT3 (Transcription factor) was observed (Fig 9C). Inhibition of EGFR by PD153035 or CHM-09 decreased the phosphorylation of AKT, ERK and STAT3 in presence of EGF, indicating that EGFR blocking leads to abrogation of downstream signalling pathways (Fig 9C). Use of specific pathway blockers decreased activation of these signalling mediators. Next to confirm if the downstream signalling pathways of EGFR holds true in CD24⁻/CD44⁺-breast CSCs, we evaluated the EGF-induced proliferation in combination of EGFR inhibitor and other pathway blockers. Indeed, EGF-induced increased proliferation of breast CSCs were significantly inhibited by these pathways blockers individually (Fig 9D). However, no further decrease in proliferation was observed when treated along with CHM-09 (Fig 9D). This observation suggests the role of EGFR signalling in maintenance of stemness (mammospheres, etc.) in breast CSCs.

EGFR inhibition suppresses EGF-induced breast CSC properties –mammosphere formation and migration: The stemness property of breast CSCs are often evaluated using an *in vitro* assay system, wherein these breast CSCs are enriched in suspension cultures as ‘mammospheres’ that imitate *in vivo* tumors [24]. The breast CSCs sorted from *MDA-MB-231*

(Fig 10A, 10B and 10C), *BT-549* (Fig 10D, 10E and 10F), *MDA-MB-453* and *MDA-MB-468* (data not shown) when treated with EGF (10ng/ml) depicted significantly larger size mammospheres and higher sphere forming efficiency as compared with vehicle control. In contrast, the sphere forming efficiency was significantly decreased by CHM-09 in dose dependent manner in presence or absence of EGF as well as PD153035 as depicted quantitatively (Fig 10C and 10F). These findings indicated that EGF-induced *in vitro* tumor formation ability of breast CSCs was hindered by PD153035 and CHM-09, via inhibiting EGFR signalling. Metastasis, a crucial phenomenon that occurs due to high migratory potential of breast CSCs was further evaluated. A significant decrease in EGF-induced migration was observed in presence of EGFR inhibitor, PD153035 and CHM-09 in dose dependent manner (Fig 11A).

EGFR inhibition perturbs the mesenchymal differentiation phenotype of breast CSCs: CD24⁻/CD44⁺-breast CSCs possess the mesenchymal phenotype that has inherent property to differentiate into adipocytes, chondrocytes and osteoblasts when cultured in specific differentiation mediums. As described in the methods, the cells grown in chondrocyte differentiation medium stained positively with toluidine blue for detection of collagen type II. EGF treated cells depicted significantly higher staining by toluidine blue as compared to vehicle control (Fig 11B) that was inhibited by an increasing dose of CHM-09 (Fig 11B) or PD153035 (5 μ M) (Fig 11C) as evaluated quantitatively (Fig 11D). Next, for the detection of adipocytes, cells were stained with Oil red O stain which specifically stains the lipid droplets present in the mature adipocytes. Breast CSCs treated with EGF depicted more number of lipid droplets as compared to vehicle control (Fig 11E) that was reduced by increasing concentration of CHM-09 (Fig 11E) or PD153035 at 5 μ M (Fig 11F) as analyzed quantitatively (Fig 11G). Further, for osteoblast differentiation, breast CSCs were cultured in

osteoblast differentiation medium and stained with 5% silver nitrate (von Kossa staining) to detect the mineral deposits. EGF treated cells showed more mineral deposits as compared to vehicle control that was attenuated in presence of CHM-09 in a concentration dependent manner (Fig 11H) or PD153035 (5 μ M) (Fig 11I) as assessed quantitatively (Fig 11J). These results demonstrate an induction of EGFR signalling that maintains the mesenchymal phenotype of breast CSCs was effectively reduced by CHM-09 or PD153035.

Inhibition of EGFR signalling induces MET and responsiveness to anticancer drugs in breast CSCs: The epithelial marker, E-cadherin was down-regulated in EGF treated cells as compared to control (Fig 12A). EGFR inhibition in presence of PD153035 or CHM-09 led to a significant up-regulation of E-cadherin expression, indicating a gain of epithelial phenotype (Fig 12A). The EGF-induced mesenchymal markers gene expression such as vimentin and fibronectin were significantly down-regulated in presence of EGFR inhibition indicating a loss of mesenchymal phenotype (Fig 12A). Interestingly, EMT-specific transcription factors, TWIST1, ZEB2 along with adhesion molecules, ALCAM and chemokines, CXCR4 and CXCR6 depicted a marked reversal of EGF-induced gene expression in presence of EGFR inhibition (Fig 12A). Similarly at protein expression levels too, EGFR inhibition led to marked decrease in vimentin and N-cadherin along with concomitant increase in E-cadherin in breast CSCs sorted from *MDA-MB-231* (Fig 12B, left panel) and *BT-549* (Fig 12B, right panel) as well as *MDA-MB-453* (Fig 12C, left panel) and *MDA-MB-468* (Fig 12C, right panel). These results demonstrate that inhibition of EGFR signalling leads to reversal of EMT or acquisition of MET by the breast CSCs. Finally, we evaluated the proliferation of our sorted breast CSCs in presence of doxorubicin, a chemotherapeutic agent. Doxorubicin alone could not inhibit the proliferation of the breast CSCs by more than 33-38%. However, when these breast CSCs isolated from *MDA-MB-231* (Fig 13A), *BT-549* (Fig 13B), *MDA-MB-453*

(Fig 13C) and *MDA-MB-468* (Fig 13D) were treated with doxorubicin along with EGFR inhibitors, a significantly high percent of inhibition (~74%) was observed (Fig 13A). These results suggest that inhibition of EGFR signalling leads to increased responsiveness of breast CSCs to chemotherapeutics.

Discussion

Breast tumor exhibits different sub-types based on its molecular profiling such as, luminal, (type A and type B), HER-2 overexpressing, normal-like and basal-like breast cancer (TNBC) [23]. TNBC is most aggressive form of breast cancer that is associated with increased rate of recurrence and poor patient survival [25]. TNBC cell lines are negative for receptors - estrogen, progesterone and HER-2 while positive for basal markers - cytokeratin5/6 and EGFR [26]. Our study correlated well with the existing literature that a TNBC cell line, *MDA-MB-231*(basal) depicted high EGFR expression as compared to *MCF-7* (luminal). Preclinical breast cancer models and clinical studies suggest that EGFR expression is concomitant with aggressive phenotype and poor clinical outcome [27]. Furthermore, basal-like tumors do not respond to conventional cancer treatments such as chemotherapy and radiotherapy. The four classes of EGFR inhibitors used for cancer therapy are monoclonal antibodies (cetuximab), antisense oligonucleotides, antibody-based immuno-conjugates and small molecules (RTKs - erlotinib and gefitinib) [26]. These kinase inhibitors prevent auto-phosphorylation of the intracellular tyrosine kinase domain of EGFR [28]. Standard cancer chemotherapy drugs affects replication of cancer cells but EGFR inhibitors target the crucial pathways of cancer cell growth and survival [29]. Due to lack of efficacious small molecule inhibitors against EGFR with less side-effects, we have synthesized a chrysin analog, CHM-09 with enhanced binding affinity to EGFR active site confirmed by molecular docking studies and cellular thermal shift assays. Our observation matched with the previous reports

that cell viability of TNBC cells significantly reduced in presence of EGFR blockers [30]. Activation of EGFR signalling in TNBC plays a major role in cancer cell proliferation, migration, EMT and metastasis via activation of downstream signalling cascades [31]. Chrysin analog, CHM-09 treated cells depicted a decreased activation of EGFR and its downstream signalling as reported in the literature [7, 8].

Aggressive TNBC tumors possess a small population of cells with stem cell-like properties of self-renewal and differentiation capabilities known as breast CSCs [32]. Apart from these, literature suggests that breast CSCs also show enhanced migration and invasion properties that aids to metastasis [33]. Metastatic human breast CSCs owing to stem cell properties forms mammospheres [24]. The observations depicting large mammosphere forming efficiency of our sorted breast CSCs suffices this important characteristic feature of self-renewal capacity [34]. The breast CSCs bearing mesenchymal phenotype exhibit tri-lineage differentiation ability into –adipocytes, chondrocytes and osteoblasts similar to mesenchymal stem cells [35]. Cancer cells which are epithelial in nature are sensitive to chemotherapies [36]. The loss of epithelial phenotype (E-cadherin) and gain of mesenchymal phenotype (vimentin, N-cadherin and Fibronectin) leads to chemoresistance in breast CSCs due to perturbation of important signal transduction pathways [37]. Thus, molecular targeted therapies against specific signalling mediator holds high hope for survival of breast cancer patients against metastatic relapse of disease [38]. Recent literature has been suggested that chemotherapeutic drugs such as paclitaxel, salinomycin, doxorubicin and etoposide inhibit tumor growth and metastasis of CSCs with limited efficiency [17] similar to our observation of very low inhibition of proliferation in our sorted breast CSCs by doxorubicin. EGFR being an important therapeutic target and expresses high in breast CSCs as compared to cancer cells makes it a preferred molecular target to inhibit CSC metastasis and recurrence of cancer. Our

data demonstrating attenuation of EGFR signalling led to reversal of EMT or induction of MET in the breast CSCs along with increased responsiveness to chemotherapeutics when simultaneously treated with doxorubicin and EGFR inhibitors suggests an effective therapeutic approach to suppress tumorigenicity and prevent metastasis in EGFR expressing breast CSCs.

Methods

Isolation of chrysin: The air dried stem bark of *Oroxylum indicum* (a voucher specimen # BD-02/07) has been deposited in the National Herbarium, Govt. of India, Shibpur, Howrah) was crushed in to powder and extracted with cold methanol [39]. The dried methanol extract was dissolved in 150 ml water and fractionated by solvent extraction using petroleum ether, chloroform, *n*-butanol, successively (20 × 3 ml each). Both chloroform and *n*-butanol fraction on column chromatography with silica gel (60-120 mesh, Merck) eluting with PE-EtOH (7:3) gave light yellow crystals of chrysin (1.3g).

Chemical characterization of isolated chrysin: The melting point of the compound was 270°C. It was then characterised by ¹H, ¹³C NMR spectral analysis and compared with the spectral data of an authentic sample.

Spectral data of chrysin: ¹H-NMR (400 MHz, DMSO-d₆): δ 12.80 (brs, 1H), 10.89 (brs, 1H), 8.04 (dd, J=8.0, 2H), 7.59 (m, 1H), 7.54 (t-like, J= 8.0 Hz, 2H), 6.50 (d, J=2.0 Hz, 1H), 6.93 (s, 1H), 6.19 (d, J=2.0 Hz, 1H), ¹³C-NMR 400 MHz, DMSO-d₆): 181.8, 164.4, 163.2, 161.4, 157.4, 121.0, 136.9, 129.0 (2C), 126.36 (2C), 105.1, 104.0., EI-MS m/z 254 [M⁺].

Protein preparation and grid generation: The X-ray crystal structures of EGFR with low resolution have been retrieved from RCSB protein data bank (www.rcsb.org). The EGF receptors of PDB ID: 3W32, 3W33, 3POZ and 3W2R [40, 41] complexed with co-ligands have been prepared using the 'Protein Preparation Wizard' [42]. Protein has been pre-processed, optimized and minimized with force field of OPLS_2005. The prepared protein was used for grid generation using the 'Receptor Grid Generation' panel. The grid box has been defined with 15Å size from the centre of selected co-crystallized ligand.

Docking validation: The docking accuracy has been evaluated by calculating root mean square deviation (RMSD). Lower the value of RMSD, higher will be the docking accuracy and for precise glide docking the value should be < 1.0 [43]. The RMSD values were calculated by superimposing best docked poses of co-ligands on its native co-ligand are summarized in Table S1. The RMSD value of 3W32 was 0.8254, which has been found to be the lowest and chosen for docking study. All the computational work were carried out using HP Z820 Workstation running over CentOS 6.3.

Chemical synthesis of chrysin analog (CHM-09): For transformation of compound **1** to compound **3**, a mixture of **1** (0.100g, 0.393 mmole), *t*-butylbromoacetate (0.1228g, 0.393 mmole), K₂CO₃ (0.110g, 0.795mmole), and 20 ml dried acetone was stirred at room temperature for 3h and the starting material **1** was disappeared [44]. The reaction mixture was dried in rotary evaporator at 40⁰C followed by extraction with ether and the residue was subjected to column chromatography over silica gel eluate PE-EtOH (9:1) gave compound **2** (0.1250g, yield: 86%) [45]. The compound was kept in vacuum desiccator for overnight. Trifluoro acetic acid was added drop by drop to compound **2** and dried in rotary evaporator for several times and resulted compound **3** (0.0946 g, yield: 88.7%). To a solution of compound

3 (0.090g, 0.288mmol) in 15 ml of dried DMF, DCC (0.090g, 1.5eq) was added and the solution was heated at 90-95°C. After 5 mins, dopamine (0.045g, 1eq), triethyl amine (0.045g, 1.5eq) and DMAP (1mg) were added to the solution and then continued heating at 90-100°C. After 24h the compound **3** disappeared on TLC from reaction mixture and the mixture was dried under reduced pressure to a semi-solid mass. This was then suspended in minimum volume (10 ml) of distilled water and extracted with ethyl acetate (3 × 10 ml). The ethyl acetate extracts were mixed together, washed with brine and dried under reduced pressure. The residue was purified using silica gel column chromatography and eluent petroleum ether-ethylacetate (8:2 ratio) gave CHM-09(U) (0.065g yield: 43.51%) while eluent petroleum ether-ethyl acetate (7:3 ratio) obtained CHM-09 (0.030g, yield: 23.28%). The R_f value of the compound CHM-09 was 0.402 (petroleum ether:ethyl acetate, 9:1). The purified compound was then characterised by physical and spectroscopic methods and was consistent with the desired structure.

Spectral data of chrysin analog, CHM-09: N-(3,4-dihydroxyphenethyl)-2-(5-hydroxy-4-oxo-2-phenyl-4H-chromen-7-yl)oxyacetamide (CHM-09): C₂₅H₂₁NO₇; Mass (ESI-MS) m/z: 449 [M+2H]; ¹H-NMR (400 MHz, DMSO-d₆): δ_H 8.10 (2H, d, J= 6.8), 8.03 (1H, brs), 7.63–7.57 (5H, m), 7.00 (1H, s), 6.57 (1H, brs), 6.24 (1H, brs), 6.00 (brs, 2H), 4.94 (1H, brs), 4.23 (s, 2H), 3.00-2.94 (2H, m), 2.16 (2H, t, J= 7.2, 7.2). ¹³C-NMR (300 MHz, DMSO-d₆): δ_C 182.6, 166.1, 164.5, 164.0, 161.6, 157.3, 154.2, 152.9, 132.6, 132.2, 131.0 (2C), 129.6, 126.9 (2C), 122.3, 116.1, 115.2, 105.9, 105.6, 98.8, 94.1, 67.2, 41.13, 39.35.

Cytotoxic effect on proliferation: 3-(4, 5-dimethylthiazol-2-yl)-2, 5-diphenyl tetrazolium bromide assay was performed to evaluate the cytotoxicity of chrysin or chrysin analog-CHM-09, and positive controls such as EGFR inhibitors, AG1478 and PD153035 (Sigma

Aldrich, USA) at a concentration of 0.01 – 100 μ M for 48h in breast cancer cell lines: *MDA-MB-231*, *MDA-MB-453*, *MDA-MB-468*, *BT-549*, *MCF-7* as well as control cells: *HEK293* (ATCC, USA) cells as previously described [46]. Separately, cells were also treated with combination of CHM-09 and pathway blockers such as wortmannin, PD98059 or static (Sigma Aldrich, USA). IC₅₀ of all the treated drugs and compounds were calculated using GraphPad prism6.

Cellular thermal shift assay (CETSA): *MDA-MB-231* cells were treated with DMSO, EGF (25ng/ml), CHM-09, PD153035 and AG1478 at a concentration of 25 μ M for 1h at 37°C. Cells were trypsinized and harvested in 0.5mL PBS supplemented with protease inhibitors. Samples were then heated at different temperatures such as 38, 42, 46, 50 and 54°C for 3 min followed by immediate 2 cycles of freeze/thaw in liquid nitrogen and at 25°C as described earlier [19]. Cell lysates were centrifuged at 20,000g for 20 min at 4°C and supernatant with soluble protein fraction were subjected to SDS-PAGE and transferred onto a PVDF membrane, probed with antibodies EGFR and tubulin (loading control).

Effect on gene expression: Total RNA extracted from *MCF-7* and *MDA-MB-231* cells was used for cDNA synthesis (Thermo Scientific, USA). Human gene-specific forward and reverse primers of various growth factor receptors, apoptotic and cell cycle genes were utilized for semi-quantitative (RT-PCR) and quantitative real-time RT-PCR (qRT-PCR, Applied Biosystems, USA) analysis as described previously [46]. Amplification of eukaryotic 18S rRNA and β -Actin was used as an internal control. All the target gene expression was normalized to internal control and depicted as the –fold change.

Effect on protein expression: Cells treated with CHM-09 and EGFR inhibitors at different concentrations for 48h were lysed and total protein isolated was subjected to SDS-PAGE, transferred to PVDF membrane and probed with various primary antibodies followed by incubation with HRP-conjugated secondary antibodies (Abcam, USA) as described earlier [47]. Visualization was performed by using G: Box (Syngene, USA).

BrdU Cell cycle analysis: MDA-MB-231 cells treated with chrysin, CHM-09, AG1478 and PD153035 at 10 μ M concentration for 24h followed by labelling with BrdU at a final concentration of 10 μ M/10⁶ cells for 24h. Cells were fixed with 5mL of ice cold ethanol and incubated at 4°C for overnight. Ethanol fixed cells were centrifuged and cell pellet was re-dissolved in 2N HCL/Triton X-100 and incubated for 30 min to denature the DNA. Next, cells were spin down and cell pellet was re-dissolved in 0.1M sodium borate (Na₂B₄O₇, pH 8.5) to neutralize the sample followed by re-suspension in 50 μ l of 0.5% Tween 20 / 1% BSA / PBS. Cells were incubated with BrdU antibody (1 μ g/10⁶ cells) for 1h and then with secondary anti-mouse Alexa Flour 488 for 30 mins at room temperature. Cells were resuspended in 0.2mL PBS contain propidium iodide (20 μ g/mL) and samples incubated in dark for 30 min followed by analysis using flow cytometer (FlowSight, Amnis, USA) as described earlier [48].

Effect on cellular apoptosis: Apoptosis assay was performed using Annexin-FITC staining kit (Biolegend, USA) of MDA-MB-231 cells treated with chrysin, CHM-09, AG1478 and PD153035 at 10 μ M concentration for 48h as described earlier [46].

Isolation of breast CSCs by Magnetic Activated Cell Sorting (MACS): Breast CSCs were isolated from MDA-MB-231, MDA-MB-453, BT-549 and MDA-MB-468 using MACS (Miltenyi Biotec, Singapore) as described previously [49] based on absence and presence of

CD24 and CD44 cell surface markers, respectively. Cells were subjected to immunodepletion by CD24 microbeads according to manufacturer's protocol. The CD24⁻ population were further subjected to CD44 selection to isolate CD24⁻/CD44⁺ (breast CSCs). The sorted CD24⁺ and CD24⁻/CD44⁺ cell population were plated for subsequent experiments in presence and absence of CHM-09 and PD153035 for cell viability assays and gene and protein expression analysis as mentioned above.

Immunofluorescence analysis: The sorted CD24⁺ and CD24⁻/CD44⁺ cell population were plated on the glass coverslips in a 6-well plate for 24h at 37°C. Cells were then fixed with methanol for 20 mins and stained with CD24 and CD44 antibodies for 2h at room temperature. Post incubation, cells were stained with fluorochrome-conjugated secondary antibodies and images were procured using confocal microscope (Fluoview FV10i, Olympus, Australia).

Purity check of sorted populations: Expression of CD24 and CD44 in the sorted cell populations were evaluated using immunofluorescence analysis under confocal microscopy as described earlier [49]. To confirm the purity of sorted CD24⁺ and CD24⁻/CD44⁺ populations, cells were stained with CD44-PE and CD24-FITC (Biolegend, USA) monoclonal antibodies for 30 min at 4°C using flow cytometry analysis carried out with BD FACS Canto (Becton Dickonson, USA) instrument and data was analyzed using FCS Express 6 software as previously described [49].

Aldefluor assay: Expression of Aldehyde dehydrogenase (ALDH) in CD24⁺ and CD24⁻/CD44⁺ populations sorted from MDA-MB-231 was assessed using flow cytometry analysis of ALDH-based cell detection kit according to manufacturer's protocol (StemCell

Technologies, USA). Briefly, to the sorted CD24⁺ and CD24⁻/CD44⁺ populations (1×10⁶ cells/mL), a fluorescent non-toxic substrate for ALDH, BODIPY amino acetaldehyde was added that diffuses into the intact viable cells. The activity of ALDH is directly proportional to the amount of fluorescent reaction product. A specific inhibitor of ALDH, diethyl amino benzaldehyde (DEAB) was used in the flow cytometry analysis as a control that shows the specificity of the enzymatic assay as well as background fluorescence correction for the flow cytometry analysis [50].

Effect on mammosphere forming capacity of breast CSCs: CD24⁻/CD44⁺ cells were plated at a density of 1×10⁴ cells/well in 1 mL of mammosphere specific medium in pHEMA (poly hydroxyl ethyl methacrylate, Sigma-Aldrich, USA) coated plates as described previously [51]. Cells were treated with PD153035 (5μM) or CHM-09 at a concentration of 0.1, 1, 10μM in presence/absence of EGF (10ng/ml). After 7 days, the images of mammospheres were taken at 10× magnification using a microscope (Olympus IX71, Japan). The size of spheres was measured using NIH Image J software (USA).

Effect on breast CSC differentiation: The CD24⁻/CD44⁺ sorted population was seeded in 24-well plate at a density of 500 cells/well and treated with PD153035 (5μM) or CHM-09 at a concentration of 0.1 and 1μM in presence/absence of EGF (10 ng/mL). The cells were maintained in adipocyte differentiation medium (Dexamethasone - 1μM, IBMX - 0.5μM and insulin - 1000ng/ml) for 14 days. For Chondrocyte and Osteoblast differentiation, cells were maintained in Chondrocyte differentiation medium (Dexamethasone – 0.1μM, Ascorbate-2-phosphate - 50μM, ITS – 500μl, sodium pyruvate - 1mM, TGF-β-3 - 1μl, proline - 0.25mg/ml) and Osteoblast differentiation medium (Dexamethasone – 0.1μM, Ascorbate-2-phosphate - 50uM, β-glycerophosphate – 10mM) for 21 and 28 days, respectively. Post

differentiation, media was removed and stained with 300 μ l of Oil red 'O' stain for Adipocyte differentiation, Toluidine blue for Chondrocyte differentiation and Von Kossa staining for Osteoblast differentiation as described earlier [49]. Images were taken at 10 \times magnification.

Statistical analysis: Results depicted in mean \pm standard error of the mean of three or more independent experiments, which were performed in triplicates. Photomicrographs represent typical experiments reproduced at least thrice with similar results. Quantitative analysis performed using NIH image J software (USA). Statistical analyses were performed to determine the difference between treatment group and their respective controls, using one-way ANOVA in GraphPad prism version 6.05 and student's paired-t test with p values ≤ 0.05 considered significant.

Acknowledgements

AD acknowledges the funding provided by DBT, Govt. of India, Cancer Pilot Project "GAP-0514, Grant Sanction No. 6242-P65/RGCB/PMD/DBT/AMTD/2015" and CSIR, Ministry of Science and Technology, Govt of India, XIIth Five-year Plan Project # CSC-0111. SD acknowledges the funding by DBT, Govt. of India, F.No.BT/327/NE/TBP/2012. Fellowships provided by DBT, ICMR and CSIR are gratefully acknowledged by KM (DBT-SRF), ND (ICMR-SRF) and RY (CSIR-JRF). We also acknowledge the technical assistance provided by Mr. Suresh Y in assisting flow cytometric analysis and confocal imaging at CSIR-IICT. This work has pending patent application.

Author Contributions

AD – Conceived, designed and conceptualised the study, performed data analysis, manuscript writing and figures; SD – Chemical structure design and synthesis and manuscript writing;

KM – Performed the experiments, data analysis and manuscript writing; NRD, RY, KG, SS – Performed biological experiments; TD – Performed synthesis of compounds and UCD – Analysis of synthesized compounds.

References

1. Davis NM, Sokolosky M, Stadelman K, Abrams SL, Libra M, and Candido S, Nicoletti F, Polesel J, Maestro R, Assoro AD, Drobot L, Rakus D, Gizak A, Laidler P, Litewka JD, Basecke J, Mijatovic S, Ivannic DM, Montalto G, Cervello M, Fitzgerald T, Demidenko Z, Martelli AM, Cocco L, Steelman LS & McCubrey JA (2014) Deregulation of the EGFR/PI3K/PTEN/AKT/mTORC1 pathway in breast cancer: possibilities for therapeutic intervention. *Oncotarget* 5, 4603-4650.
2. Takeuchi K & Ito F (2011) Receptor tyrosine kinases and targeted cancer therapeutics. *Biol Pharm Bull* 34, 1774-1780.
3. Wendt MK, Jason A, Smith BS & Schiemann WP (2010) Transforming Growth Factor- β -induced Epithelial-Mesenchymal Transition facilitates epidermal growth factor-dependent breast cancer progression. *Oncogene* 29, 6485-6498.
4. Hicklin DJ & Ellis LM (2005) Role of the vascular endothelial growth factor pathway in tumor growth and angiogenesis. *J Clin Oncol* 23, 1011-1027.
5. Ball SG, Shuttleworth A & Kielty C (2012) Inhibition of platelet-derived growth factor receptor signalling regulates oct4 and nanog expression, cell shape, and mesenchymal stem cell potency. *Stem Cells* 30, 548-560.
6. Wang J, Barnes RO, West NR, Olson M, Chu JE & Watson PH (2008) Jab1 is a target of EGFR signalling in ER α -negative breast cancer. *Breast Cancer Res* 10, 1-11.
7. Christopher P, Michael D, Michael S, Settleman J, James FL & David J R (2011) ErbB2 is necessary for ErbB4 ligands to stimulate oncogenic activities in models of human breast cancer. *Genes & Cancer* 2, 792-804.
8. Corkery B, Crown J, Clynes M & Donovan N (2009) Epidermal growth factor receptor as a potential therapeutic target in triple-negative breast cancer. *Annals Oncol* 20, 862-867.
9. Rimawi F, Shetty B, Weiss H, Schiff R, Osborne K, Chamness G & Elledge M (2010) EGFR expression in breast cancer association with biologic phenotype and clinical outcomes. *Cancer* 116, 1234-1242.

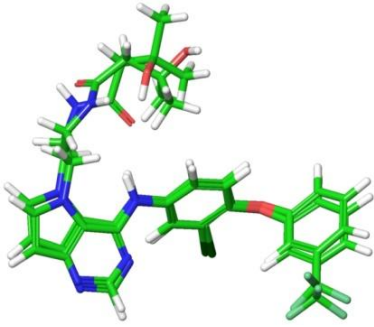
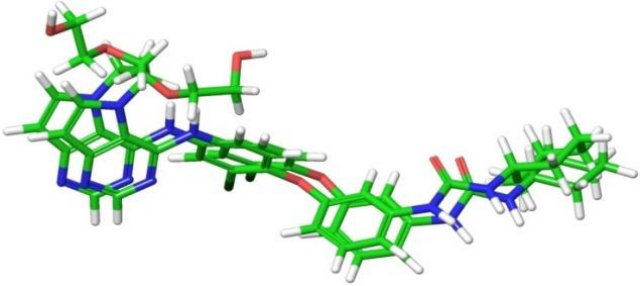
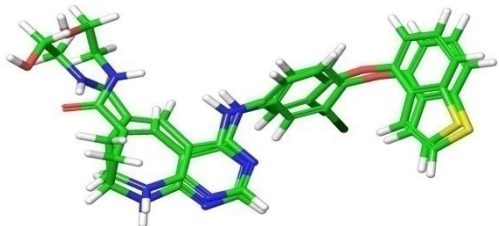
- Accepted Article
10. John T, Tony T, Agarwal A, Djakiew D & Thompson W (1999) Epidermal growth factor promotes MDA-MB-231 breast cancer cell migration through a phosphatidylinositol 3-kinase and phospholipase c-dependent mechanism. *Cancer Res* 59, 5475–5478.
 11. Zhang D, Tari A, Akar U, Arun B, LaFortune A, Nieves-Alicea R & Ueno NT (2010) Silencing kinase interacting stathmin gene enhances erlotinib sensitivity by inhibiting serine 10 p27 phosphorylation in EGFR expressing breast cancer. *Mol Cancer Ther* 9, 3090-3099.
 12. Choowongkamon K, Sawatdichaikul O, Songtawee N & Limtrakul J (2010) Receptor-based virtual screening of EGFR kinase inhibitors from the NCI diversity database. *Molecules* 15, 4041-4054.
 13. Kasala E, Boddulure BL, Madana RM, Athira K V, Gogoi R & Barua C (2015) Chemopreventive and therapeutic potential of chrysin in cancer: mechanistic perspectives. *Toxicol Lett* 233, 214-225.
 14. Walle T, Otake Y, Brubaker JA, Walle UK & Halushka PV (2001) Disposition and metabolism of the flavonoid chrysin in normal volunteers. *Br J Clin Pharmacol* 51, 143–146.
 15. Zheng H, Li S, Pu Y, Lai Y, He B & Gu Z (2014) Nanoparticles generated by PEG-chrysin conjugates for efficient anticancer drug delivery. *Eur J Pharm Biopharm* 7, 454-460.
 16. Liu S & Wicha MS (2010) Targeting breast cancer stem cells. *J Clin Oncol* 28, 4006-4012.
 17. Gupta B, Tamer T, Jiang, G, Tao K, Kuperwasser C, Weinberg A & Lander E (2009) Identification of selective inhibitors of cancer stem cells by high-throughput screening. *Cell* 138, 645-659.
 18. Switzer CH, Glynn SA, Cheng RYS, Ridnour LA, Green JE, Ambs S & Wink DA (2012) S-Nitrosylation of EGFR and Src activates an oncogenic signalling network in human basal-like breast cancer. *Mol Cancer Res* 10, 1203-1215.
 19. Jafari R, Almqvist H, Axelsson H, Ignatushchenko M, Lundback T, Nordlund P & Molina DM (2014) The cellular thermal shift assay for evaluating drug target interactions in cells. *Nature Protocol* 9, 2100-2122.
 20. Phuc V Pham PV, Phan NLC, Nguyen N, Truong NH, Duong TT, Le DV, Truong KD & Phan NK (2011) Differentiation of breast cancer stem cells by knockdown of CD44: promising differentiation therapy. *J Translational Med* 9, 1-13.

21. Fang D, Hawke D, Zheng Y, Xia Y, Meisenhelder J, Nika H, Mills GB, Kobayashi R, Hunter T & Lu Z (2007) Phosphorylation of β -catenin by AKT promotes β -catenin transcriptional activity. *J Biol Chem* 282, 11221-11229.
22. Marotta LLC, Almendro V, Marusyk A, Shipitsin M, Schemme J, Walker SR, Qimron NB, Kim JJ, Choudhury SA, Maruyama R, Wu Z, Gonen M, Mulvey LA, Bessarabova MO, Huh SJ, Silver SJ, Kim SY, Park SY, Lee HE, Anderson KS, Richardson AL, Nikolskaya T, Nikolsky Y, Liu S, Root DE, Hahn WC, Frank DA & Polyak K (2011) The JAK2/STAT3 signalling pathway is required for growth of CD44⁺CD24⁻ stem cell-like breast cancer cells in human tumors. *J Clin Invest* 121, 2723-2735.
23. Tischkowitz M, Brunet JS, Begin LR, Huntsman DG, Cheang MCU, Akslen LA, Nielsen TO & Foulkes WD (2007) Use of immunohistochemical markers can refine prognosis in triple negative breast cancer. *BMC Cancer* 7, 1-11.
24. Grimshaw M, Cooper L, Papazisis K, Coleman JL, Bohenkamp HR, Stanke LC, Papadimitriou JT & Burchell JM (2008) Mammosphere culture of metastatic breast cancer cells enriches for tumorigenic breast cancer cells. *Breast Cancer Res* 10, 1-10.
25. Ovcaricek T, Frkovic SG, Matos E, Mozina B & Borstnar S (2011) Triple negative breast cancer -prognostic factors and survival. *Radiol Oncol* 45, 46-52.
26. Bauer KR, Brown M, Cress RD, Parise CA & Caggiano V (2007) Descriptive analysis of estrogen receptor (ER)-negative, progesterone receptor (PR)-negative, and her2-negative invasive breast cancer, the so-called triple-negative phenotype. *Cancer* 109, 1721-1728.
27. Teng YHF, Tan WJ, Thike AA, Cheok PY, Tse GMK, Wong NS, Yip GW, Bay BH & Tan PH (2011) Mutations in the epidermal growth factor receptor (EGFR) gene in triple negative breast cancer: possible implications for targeted therapy. *Breast Cancer Res* 13, 1-9.
28. Bachawal SV, Wali VB & Sylvester PW (2010) Enhanced antiproliferative and apoptotic response to combined treatment of gamma-tocotrienol with erlotinib or gefitinib in mammary tumor cells. *BMC Cancer* 10, 1-13.
29. Ciardiello F & Tortora G (2001) A novel approach in the treatment of cancer: targeting the epidermal growth factor receptor. *Clin Cancer Res* 7, 2958-2970.
30. Lacouture ME (2006) Mechanisms of cutaneous toxicities to EGFR inhibitors. *Cancer* 6, 803-812.

31. Yang L, Li Y, Ding Y, Choi KS, Kazim AL & Zhang Y (2013) Prolidase directly binds and activates epidermal growth factor receptor and stimulates downstream signalling. *J Biol Chem* 288, 2365-75.
32. Jin W, Chen B, Li J, Zhu H, Huang M, Gu SM, Wang QQ, Chen JY, Yu S, Wu J & Shao ZM (2012) TIEG1 inhibits breast cancer invasion and metastasis by inhibition of epidermal growth factor receptor (EGFR) transcription and the egfr signalling pathway. *Mol Cell Biol* 32, 50-63.
33. Stratford A, Habibi G, Astanehe A, Jiang H, Hu K, Park E, Shadeo A, Buys TP, Lam W, Pugh T, Marra M, Nielsen TO, Klinge U, Mertens PR, Aparicio S & Dunn SE (2007) Epidermal growth factor receptor (EGFR) is transcriptionally induced by the Y-box binding protein-1 (YB-1) and can be inhibited with Iressa in basal-like breast cancer, providing a potential target for therapy. *Breast Cancer Res* 9, 1-14.
34. Alam M, Rajabi H, Ahmed R, Jin C & Kufe D (2014) Targeting the MUC1-C oncoprotein inhibits self-renewal capacity of breast cancer cells. *Oncotarget* 5, 2622-2634.
35. Battula VL, Evas KW, Hollier BG, Shi Y, Marini FC, Ayyanan A, Wang RY, Brisken C, Guerra R, Andreeff M & Mani SA (2010) Epithelial-mesenchymal transition-derived cells exhibit multi-lineage differentiation potential similar to mesenchymal stem cells. *Stem Cells* 28, 1435-1445.
36. Sajithlal G, Rothermund K, Zhang F, Dabbs DJ, Latimer JJ, Grant SG & Prochownik EV (2010) Permanently blocked stem cells derived from breast cancer cell lines. *Stem Cells* 28, 1008-1018.
37. Fillmore CM & Kuperwasser C (2008) Human breast cancer cell lines contain stem-like cells that self-renew, give rise to phenotypically diverse progeny and survive chemotherapy. *Breast Cancer Res* 10, 1-13.
38. Qin L, Liu Z, Chen H & Xu J (2009) The steroid receptor coactivator-1 regulates twist expression and promotes breast cancer metastasis. *Cancer Res* 69, 3819-3827.
39. Dinda B, Mohanta BC, Arima S, Sato N & Harigaya Y (2007) Flavonoids from the stem-bark of *Oroxylum indicum*. *Nat Prod Sci* 13,190-194.
40. Aertgeerts K, Skene R, Yano J, Sang BC, Zou H, Snell G, Jennings A, Iwamoto K, Habuka N, Hirokawa A, Ishikawa T, Tanaka T, Miki H, Ohta Y & Sogabe S(2011) Structural analysis of the mechanism of inhibition and allosteric activation of the kinase domain of HER2 protein. *J Biol Chem* 286, 18756-18765.

41. Kawakita Y, Seto M, Ohashi T, Tamura T, Yusa T, Miki H, Iwata H, Kamiguchi H, Tanaka T, Sogabe S, Ohta Y & Ishikawa T (2013) Design and synthesis of novel pyrimido [4,5-b]azepine derivatives as HER2/EGFR dual inhibitors. *Bioorg. Med. Chem* 21, 2250–2261.
42. Schrödinger Suite (2013) Protein Preparation Wizard; Epik version 2.5, Schrödinger, LLC, New York, NY.
43. Loving K, Salam NK & Sherman W (2009) Energetic analysis of fragment docking and application to structure-based pharmacophore hypothesis generation. *J Comp Aided Mol Des* 23, 541–554.
44. Christian AGN, Montalbetti & Falque V (2005) Amide bond formation and peptide coupling. *Tetrahedron* 61, 10827–10852.
45. Hu K, Wang W, Cheng H, Pan S & Ren J, (2011) Synthesis and cytotoxicity of novel chrysin derivatives. *Med Chem Res* 20, 838-846.
46. Geesala R, Gangasani JK, Budde M, Balasubramanian S, Vaidya JR & Das A (2016) 2 Azetidiones: Synthesis and biological evaluation as potential anti-breast cancer agents. *Eur J Med Chem* 124, 554-558.
47. Das A, Fernandez-zapico ME, Cao S, Yao J, Fiorucci S, Hebbel RP, Urrutia R & Shah V (2006) Disruption of a sp2/klf6 repression complex by SHP is required for farnesoid x receptor-induced endothelial cell migration. *J Biol Chem* 281, 39105-39113.
48. Wei Lin D, Chung BP & Kaiser P (2014) S-adenosylmethionine limitation induces p38 mitogen-activated protein kinase and triggers cell cycle arrest in G1. *J Cell Sci* 127, 50-59.
49. Dhoke NR, Kalabathula E, Kaushik K, Geesala R, Sravani B & Das A (2016) Histone deacetylases differentially regulate the proliferative phenotype of mouse bone marrow stromal and hematopoietic stem/progenitor cells. *Stem Cell Res* 17, 170-180.
50. Jauffret E, Ginestier C, Iovino F, Tarpin C, Diebel M, Esterni B, Houvenaeghel G, Extra JM, Bertucci F, Jacquemier J, Xerri L, Dontu G, Stassi G, Xiao Yi, Barsky S, Birnbaum D, Viens P & Wicha MS (2010) ALDH1-positive cancer stem cells mediate metastasis and poor clinical outcome in inflammatory breast cancer. *Clin Cancer Res* 16, 45-55.
51. Vinnedge LMP, McClaine R, Wagh PK, Brokamp KAW, Waltz SE & Wells SI (2011) The human DEK oncogene stimulates beta catenin signalling, invasion and mammosphere formation in breast cancer. *Oncogene* 30, 2741-2752.

Table 1. The RMSD values of different EGFR

| Sl. No | PDB ID | Superposition of docked co-ligand on its originally bound native conformation of co-ligand in X-ray ligand-enzyme complex | Resolution [Å] | RMSD |
|--------|--------|---|----------------|--------|
| 1 | 3POZ |  | 1.50 | 1.4900 |
| 2 | 3W2R |  | 2.05 | 2.3100 |
| 3 | 3W32 |  | 1.80 | 0.8254 |
| 4 | 3W33 |  | 1.70 | 1.1633 |

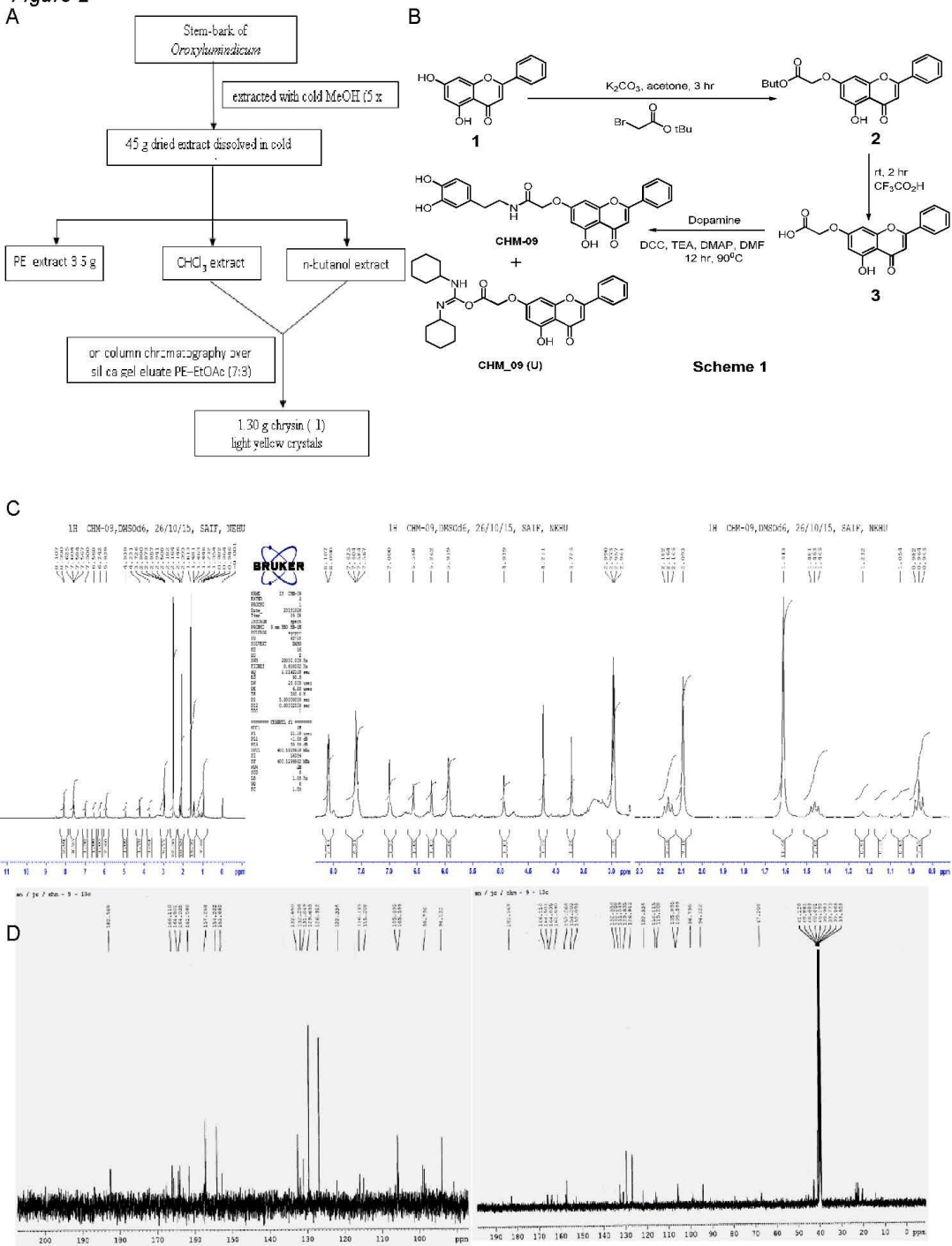
Supporting Information

Figure S1: Representative western blot analysis of EGFR expression in CD24⁺ and CD24⁻/CD44⁺ cells depicting relatively high expression of EGFR in CD24⁻/CD44⁺ cells.

Table S1: List of Primers sequence of cell cycle, apoptosis and EMT specific markers.

Figure 1. Molecular docking of chrysin analogs of EGFR: High expression of EGFR in *MDA-MB-231* than *MCF-7* as observed by (A) semi-quantitative RT-PCR and (B) immunoblotanalysis. Chemical structure of (C) chrysin and (D) its analog, CHM-09. Molecular docking of EGFR with CHM-09 as depicted by (E) 2-D ligand interaction, (F) 2D ligand interaction diagram of a co-ligand and CHM-09 receptor (PDB ID: 3W32). PDB ID: 3W32, co-ligand ID: W32, XPGS: -14.297, Interacting amino acid residues: HBD: MET-793, HBA: MET-793, HPB: PHE-856 (G) 3-D hydrogen bond donor, hydrogen bond acceptor and (H) hydrophobic interaction with active site amino acid residues.

Figure 2

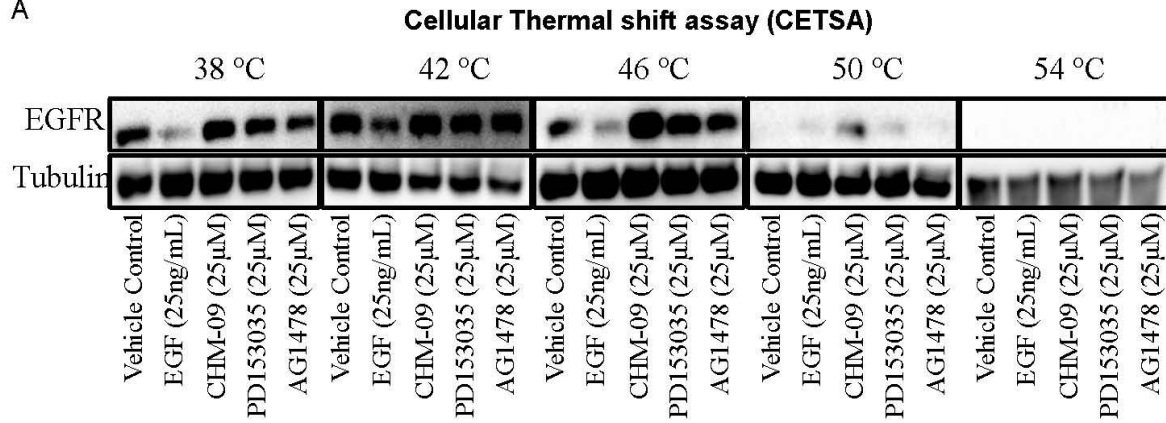


Accepted Article

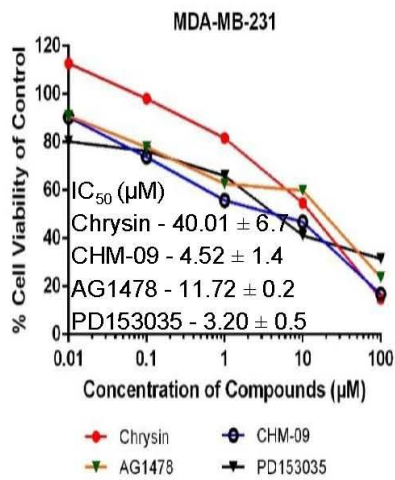
Figure 2. Isolation of chrysin, its analog synthesis and chemical characterization: (A) Schematic representation of isolation of chrysin from *Oroxylum indicum*. (B) Schematic representation of chrysin analog, CHM-09 synthesis. Spectral analysis of the synthesized chrysin analog, CHM-09 using (C) ^1H NMR (D) ^{13}C NMR.

Figure 3

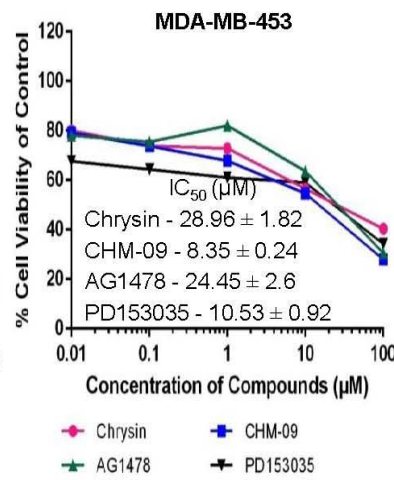
A



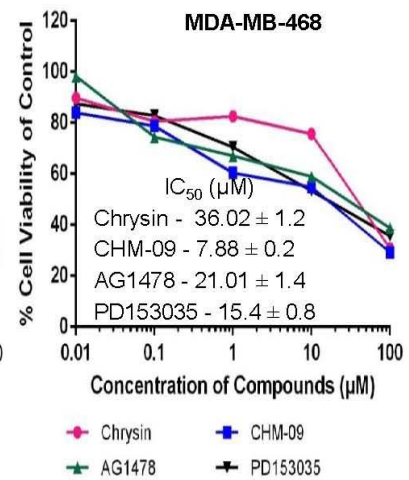
B



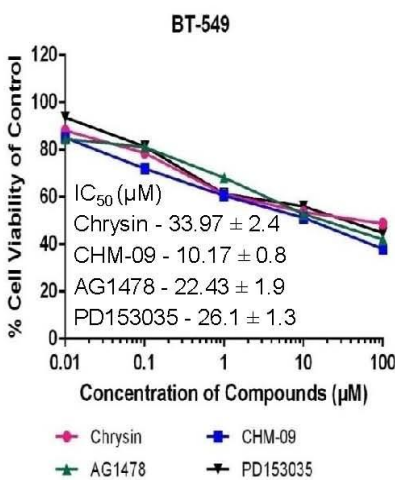
C



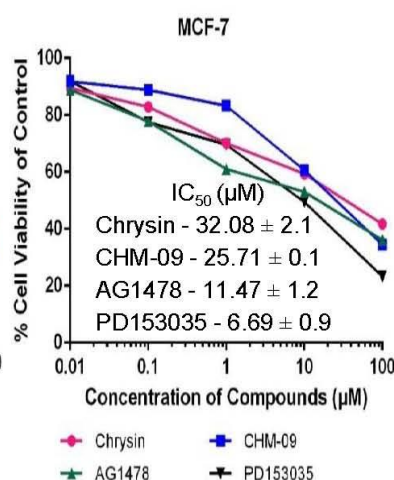
D



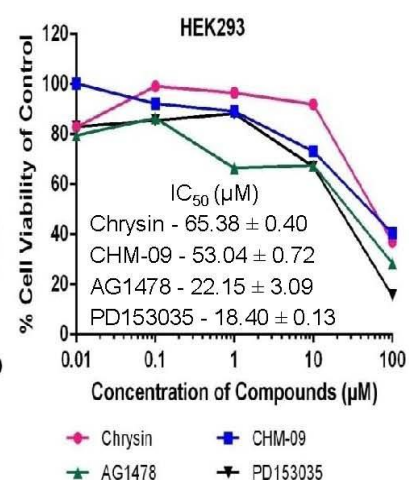
E



F



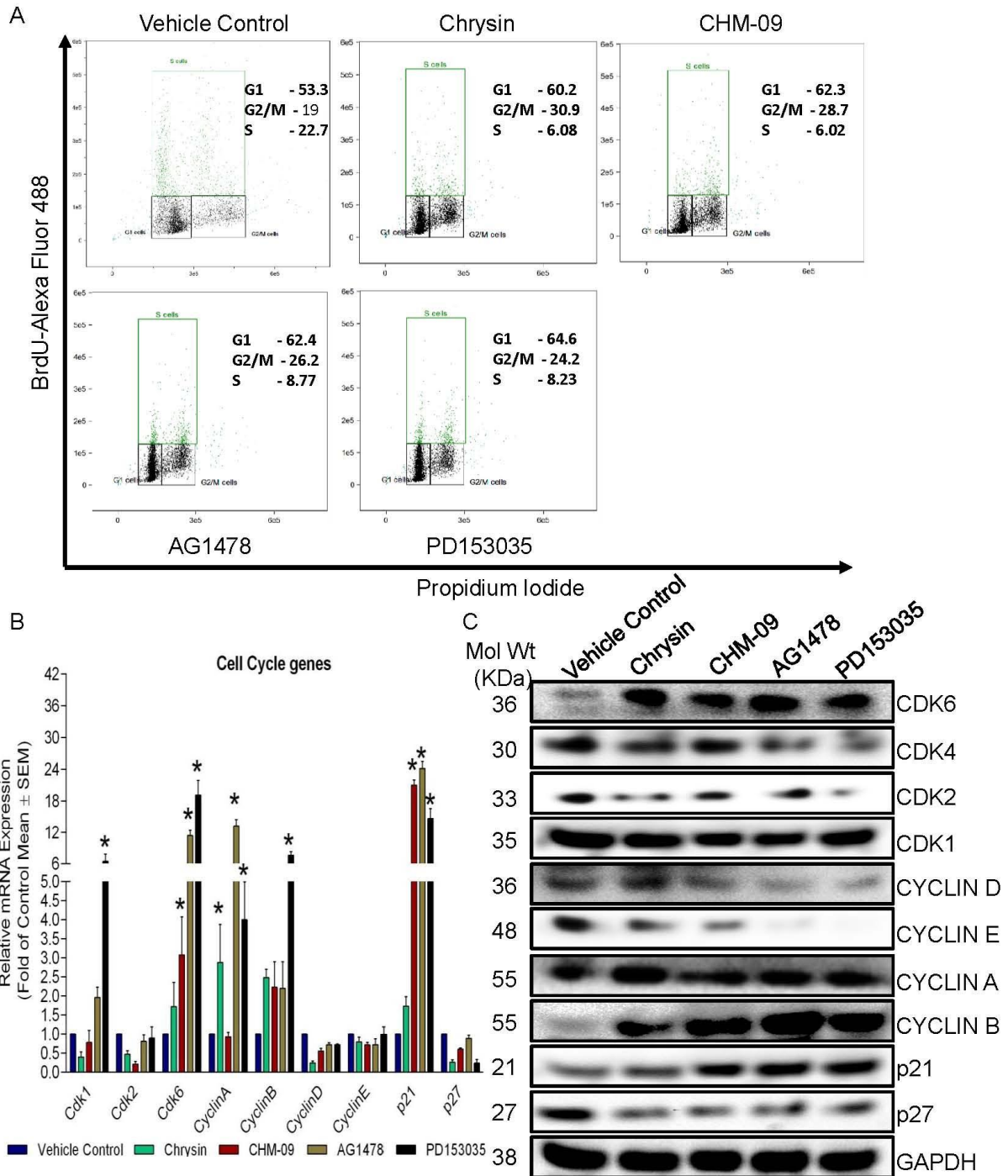
G



Accepted Article

Figure 3. EGFR inhibition-mediated modulation of cell viability in TNBCs: (A) MDA-MB-231 cells treated with different inhibitors at high concentrations as depicted in the figure for 1h at 37°C, followed by trypsinization of cells and exposing them to different temperatures for 3 mins. Cell lysates were then subjected to immunoblot analysis as described in methods. Cellular thermal shift assay depicting stabilization of EGFR in presence of CHM-09 at high temperature (50°C) indicating that CHM-09 binding to EGFR (n=3). Cell viability in presence of CHM-09 (0.01-100µM, for 48h) depicted a marked low IC₅₀ values in (B) MDA-MB-231 (C) MDA-MB-453 (D) MDA-MB-468 and (E) BT-549 as compared to (F) MCF-7 (n=4). (G) CHM-09 (0.01-100µM, for 48h) depicted low cytotoxicity (high IC₅₀) to primary control cells, HEK293 as compared to standard EGFR inhibitors (n=4). Data represented mean of four independent experiments. IC₅₀ (µM) is represented in mean ± SEM.

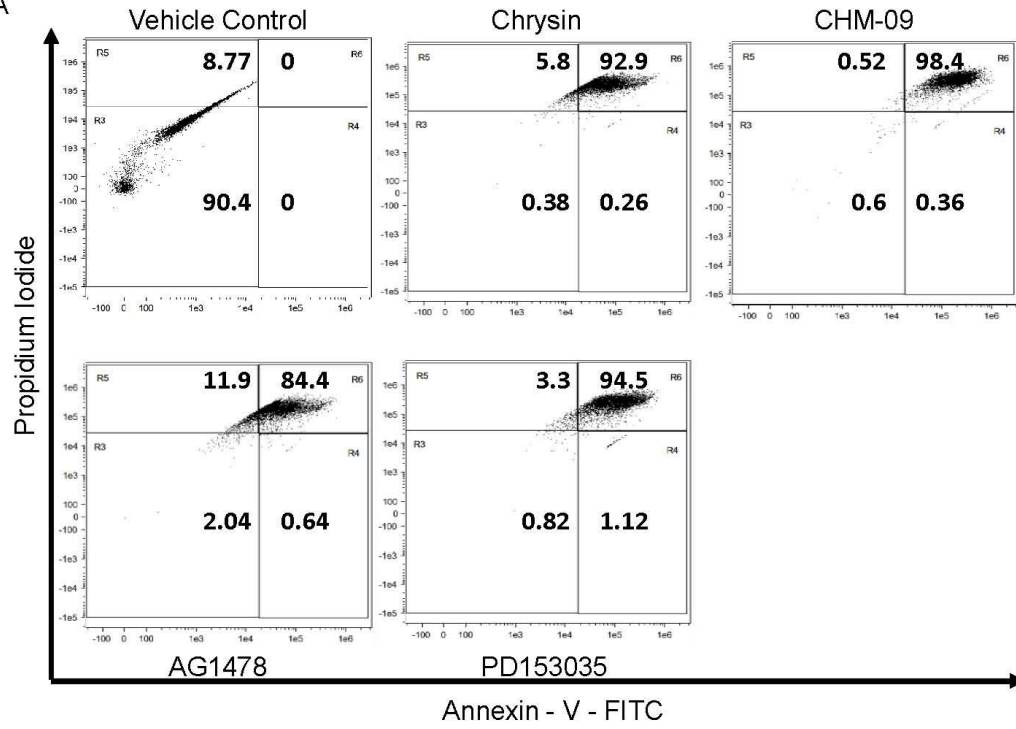
Figure 4



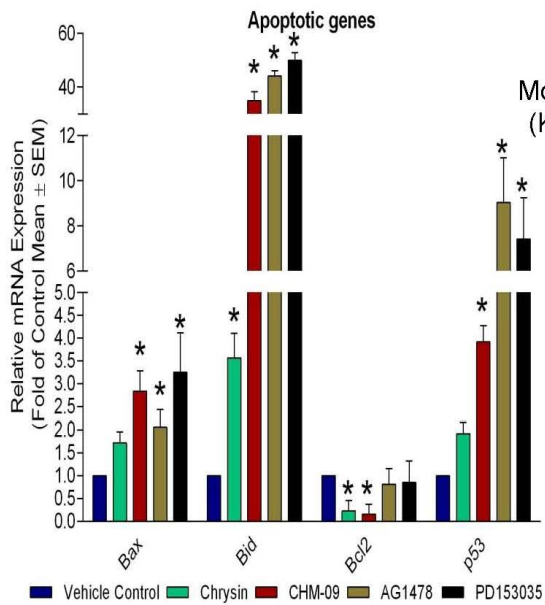
*Figure 4. EGFR inhibitors intervene cell cycle in TNBCs: MDA-MB-231 cells were treated with chrysin, CHM-09, AG1478 and PD153035 at a concentration of 10 μ M for 48h. (A) Flow cytometric analysis of BrdU cell cycle depicted a G₀/G₁ arrest by chrysin, CHM-09, AG1478 and PD153035 (n=3). (B) qRT-PCR analysis of cell cycle genes represented differential expression of cyclins, CDKs and CKIs (n=3). (C) Representative image of western blot analysis of cell cycle regulators depicting decreased cyclins D and E along with CDK2 and 4 indicating G₀/G₁ arrest by CHM-09 and EGFR inhibitors in *MDA-MB-231* cells. Data are the mean \pm SEM of at least three independent experiments. *p < 0.05 (*t*-test) as compared to vehicle control.*

Figure 5

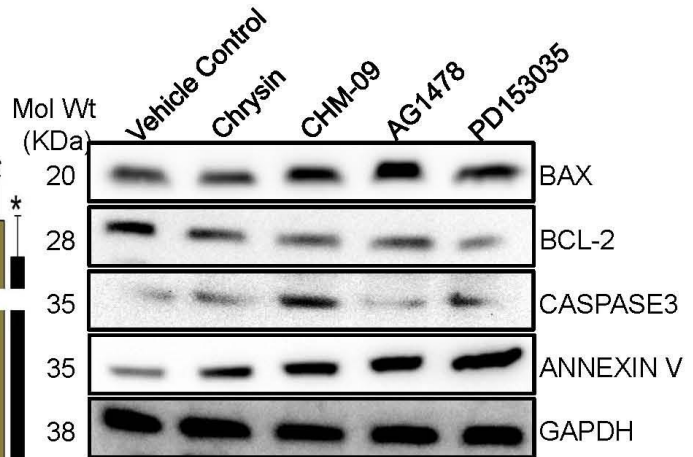
A



B



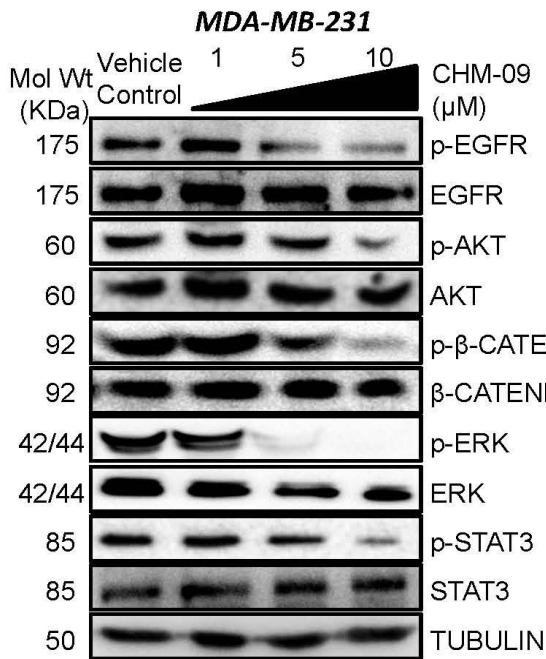
C



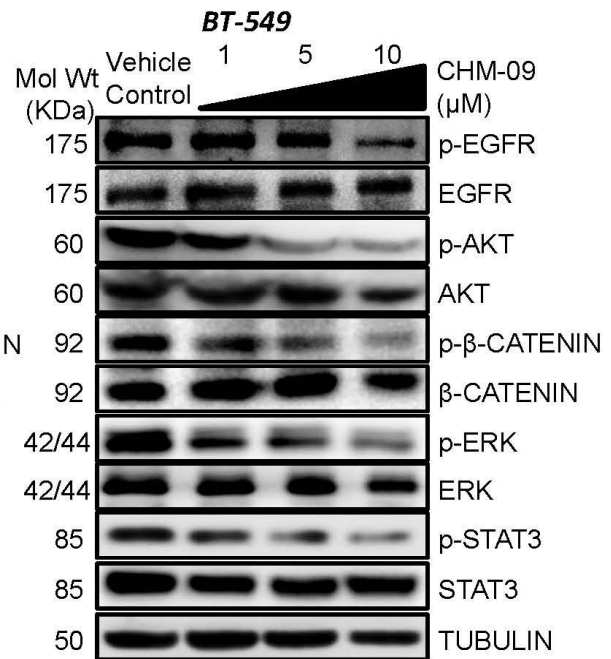
*Figure 5. EGFR inhibitors induces apoptosis in TNBCs: MDA-MB-231 cells were treated with chrysin, CHM-09, AG1478 and PD153035 at a concentration of 10 μ M for 48h. (A) Flow cytometric analysis using annexin-FITC/PI staining revealed a marked increase in late apoptotic cells with CHM-09 treatment (n=3). (B) Relative mRNA expression levels of apoptotic genes depicted a significant upregulation of pro-apoptotic genes whereas downregulation of anti-apoptotic gene (n=3). (C) Representative photomicrograph of western blot analysis of apoptotic proteins depicted high expression of apoptotic proteins –Bax, Caspase3 and Annexin V in presence of inhibitors and CHM-09 as compared to control. Data are the mean \pm SEM of three independent experiments with at least triplicate samples, *p < 0.05 (*t*-test) as compared to control.*

Figure 6

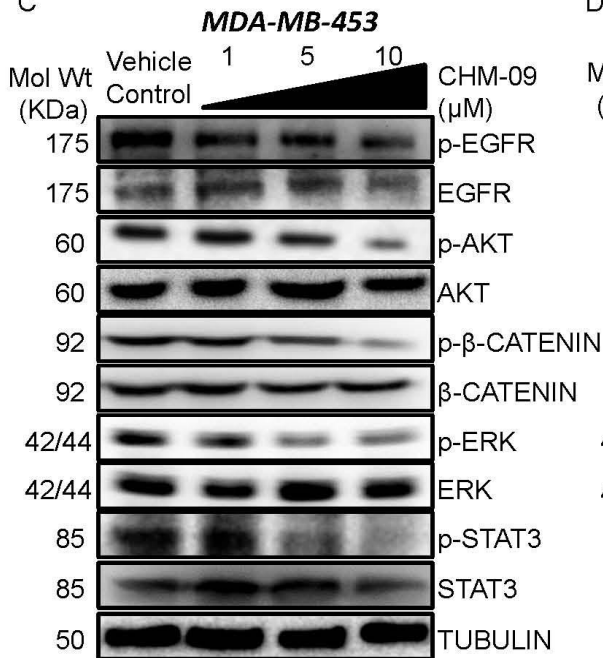
A



B



C



D

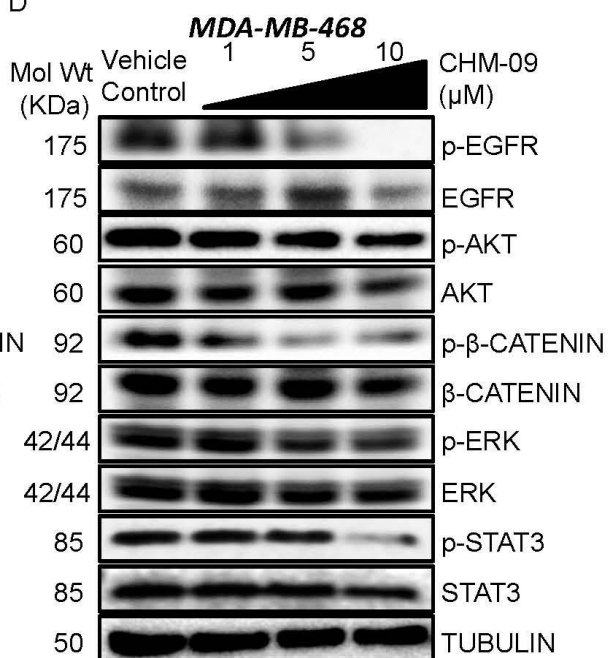


Figure 6. EGFR inhibition regulates downstream signalling in TNBCs: Representative photomicrographs of immunoblot analysis of (A) *MDA-MB-231*, (B) *BT-549* (C) *MDA-MB-453* and (D) *MDA-MB-468* cells treated with increasing concentrations (1-10 μ M) of CHM-09 for 48h depicted attenuation of EGFR downstream signalling mediators, AKT, ERK and STAT3. Data represented are from experiments repeated at least thrice (n=3).

Figure 7

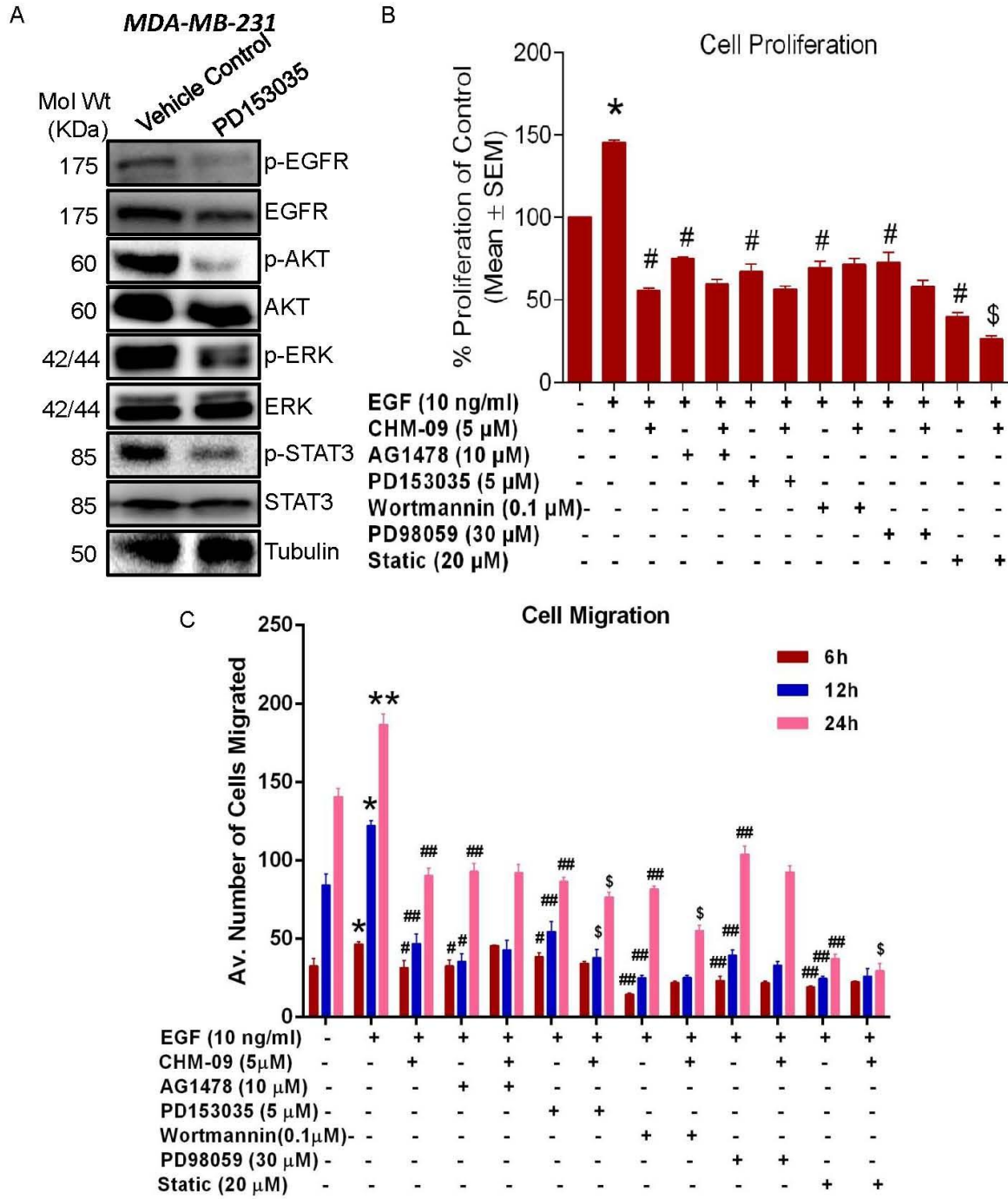
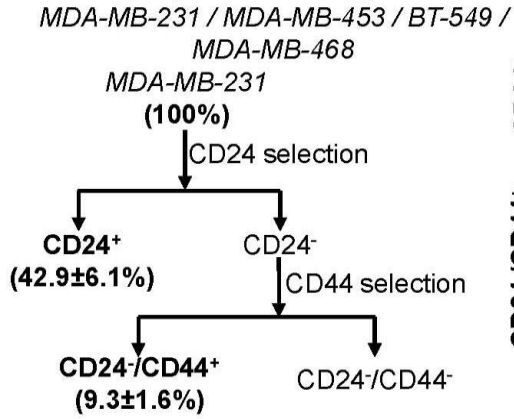


Figure 7. EGFR downstream signalling regulates TNBCs cell proliferation and migration:

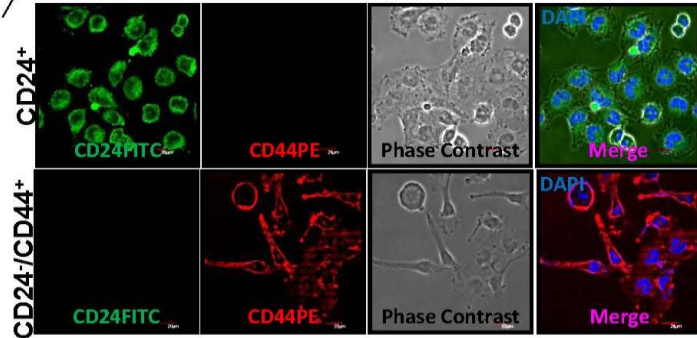
(A) Representative image of immunoblot analysis of EGFR signalling in *MDA-MB-231* cells treated with PD153035 at a concentration of 5 μ M. Pathway-specific inhibitors in presence or absence of CHM-09 depicted significant decrease in (B) cell proliferation (n=6) and (C) cell migration (n=4). Data are the mean \pm SEM of three independent experiments, $p \leq 0.05$ (*t*-test) as compared to *control and #EGF-treated group.

Figure 8

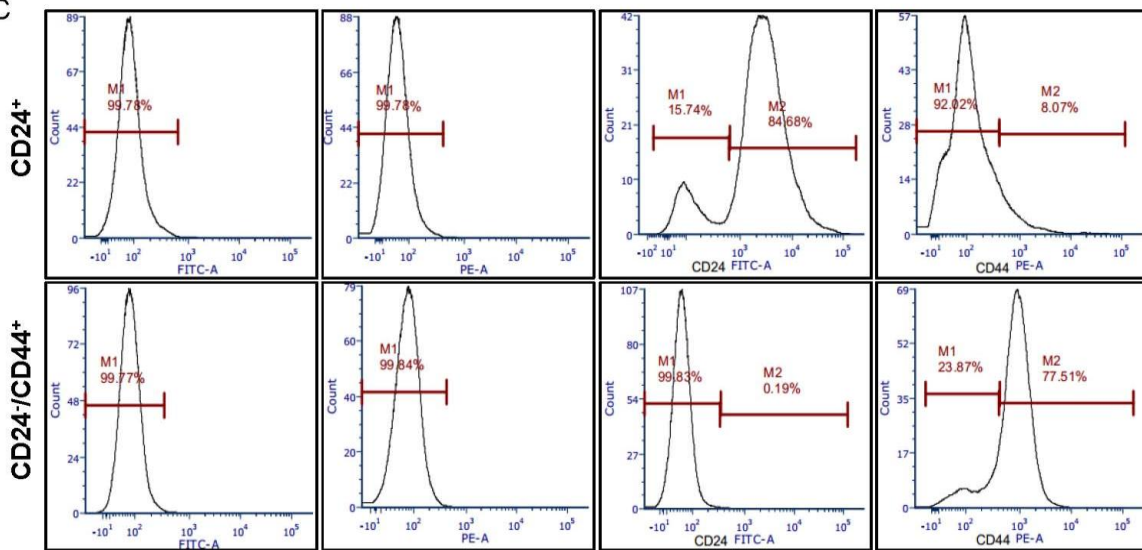
A Breast Cancer Stem Cells Isolation
(% Yield of total)



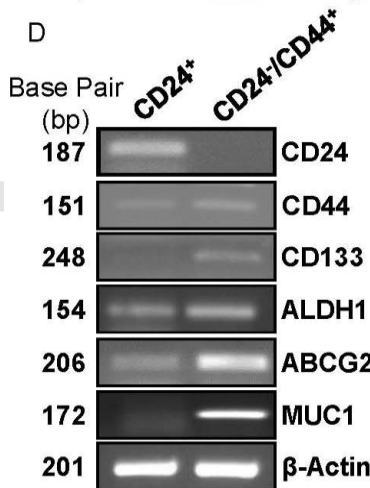
B



C



D



E

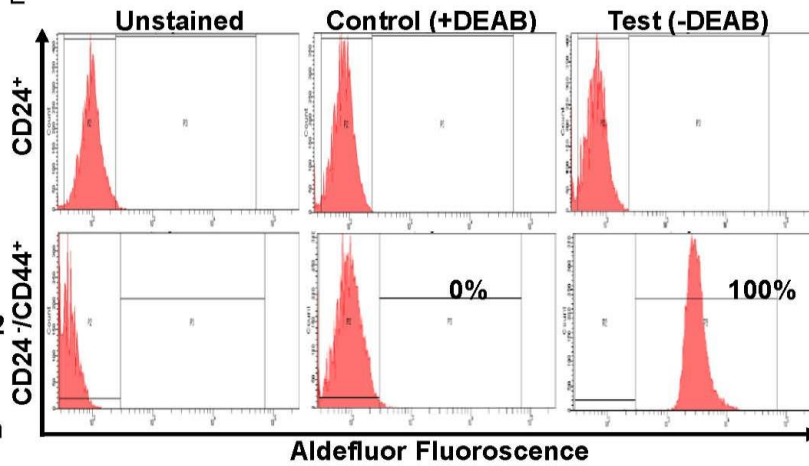
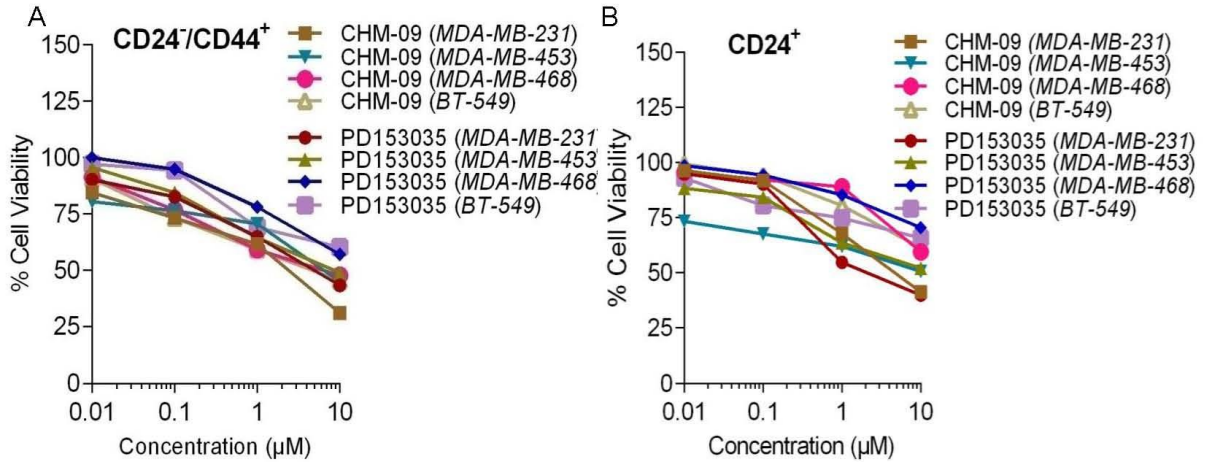


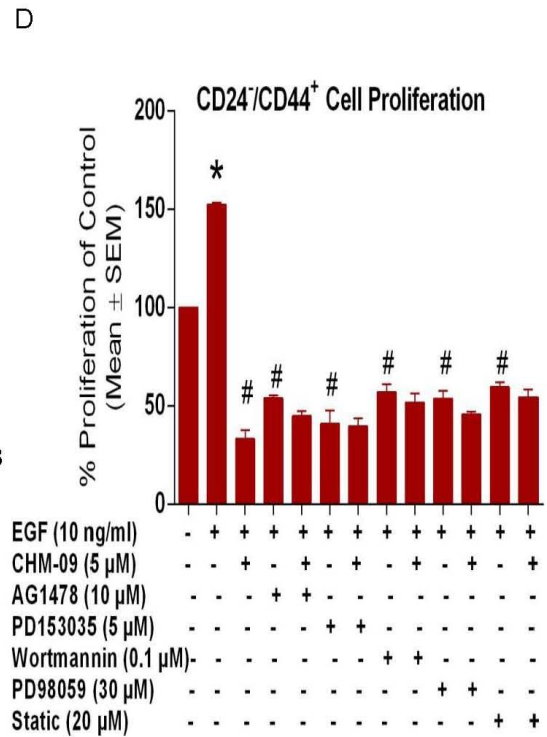
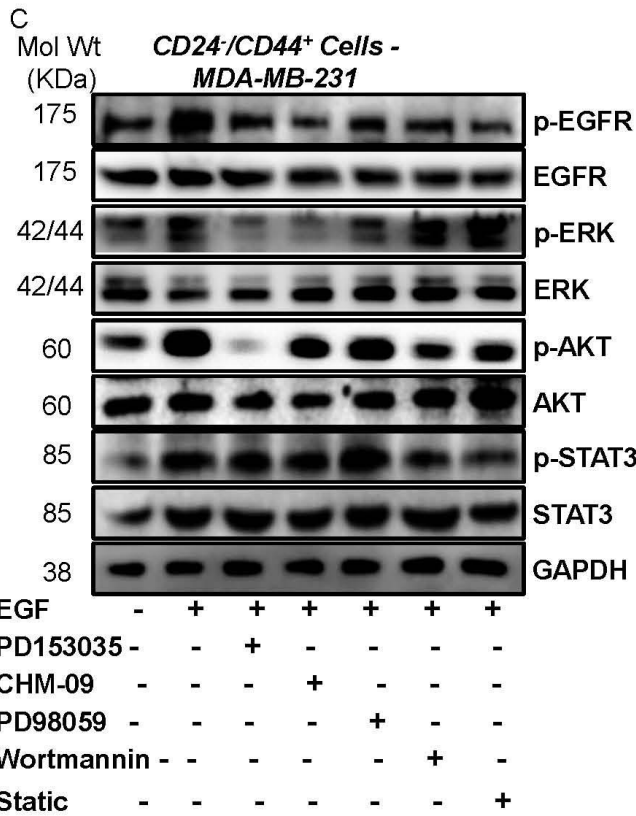
Figure 8. Isolation and characterization of breast CSCs from TNBCs: (A) Flow chart of breast CSCs sorting from *MDA-MB-231*, *BT-549*, *MDA-MB-453* and *MDA-MB-468* cells using MACS. The value in parenthesis represents the percent yield of total cells. (B) Confocal images of $CD24^+$ and $CD24^-/CD44^+$ cells depicting expression of CD24 and CD44 markers in sorted populations of cancer cells and CSCs, respectively. Scale bars: 20 μ m. (C) Purity check of sorted populations using flow cytometric analysis depicted that CSCs ($CD24^-/CD44^+$) exhibited 77.5% and 0.19% positive for CD44 and CD24, respectively whereas cancer cells ($CD24^+$) were 84.68% positive for CD24 and 8.07% for CD44. (D) Semi-quantitative RT-PCR results depicted differential expression of CSC-specific genes in $CD24^+$ -breast cancer cells and $CD24^-/CD44^+$ -breast CSC. (E) ALDH assay depicting 100% aldefluor fluorescence in CSCs indicating these sorted populations to be $ALDH^+$ (n=3). Data depicted are representative results obtained from experiments repeated at least six times.

Figure 9



| TNBC Cell lines | IC ₅₀ (μM) CD24 ⁺ /CD44 ⁺ | |
|-----------------|--|----------|
| | CHM-09 | PD153035 |
| MDA-MB-231 | 1.3±0.4 | 2.2±0.6 |
| MDA-MB-468 | 3.2±0.1 | 11.5±0.5 |
| MDA-MB-453 | 6.1±0.3 | 10.7±0.1 |
| BT-549 | 4.3±0.3 | 17.6±1.0 |

| TNBC Cell lines | IC ₅₀ (μM) CD24 ⁺ | |
|-----------------|---|----------|
| | CHM-09 | PD153035 |
| MDA-MB-231 | 8.8±2.2 | 6.4±0.1 |
| MDA-MB-468 | 14.9±1.2 | 25.5±0.4 |
| MDA-MB-453 | 17.6±1.1 | 11.4±0.6 |
| BT-549 | 18.9±1.2 | 31.9±1.0 |



*Figure 9. EGFR-mediated regulation of cell proliferation in breast CSCs isolated from TNBCs: Proliferative potential of (A) CD24⁻/CD44⁺-breast CSCs and (B) CD24⁺-breast cancer cells sorted from a panel of TNBC cell lines –MDA-MB-231, MDA-MB-453, MDA-MB-468 and BT-549 in presence of CHM-09 and PD153035 (0.01-10 μ M, for 48h) depicted high efficacy (low IC₅₀ values) in reducing cell viability of breast CSCs as compared to cancer cells (n=6). Data represented (IC₅₀ - μ M) are mean \pm SEM of four independent experiments. p<0.05 as compared to *control and #EGF-treated group. (C) Representative image of immunoblot analysis of EGFR downstream signalling in breast CSCs in presence of specific pathway blockers and EGFR inhibitors. (D) EGFR inhibitors as well as downstream targets of EGFR signalling pathway inhibitors-mediated decrease in proliferation of breast CSCs (n=3).*

Figure 10

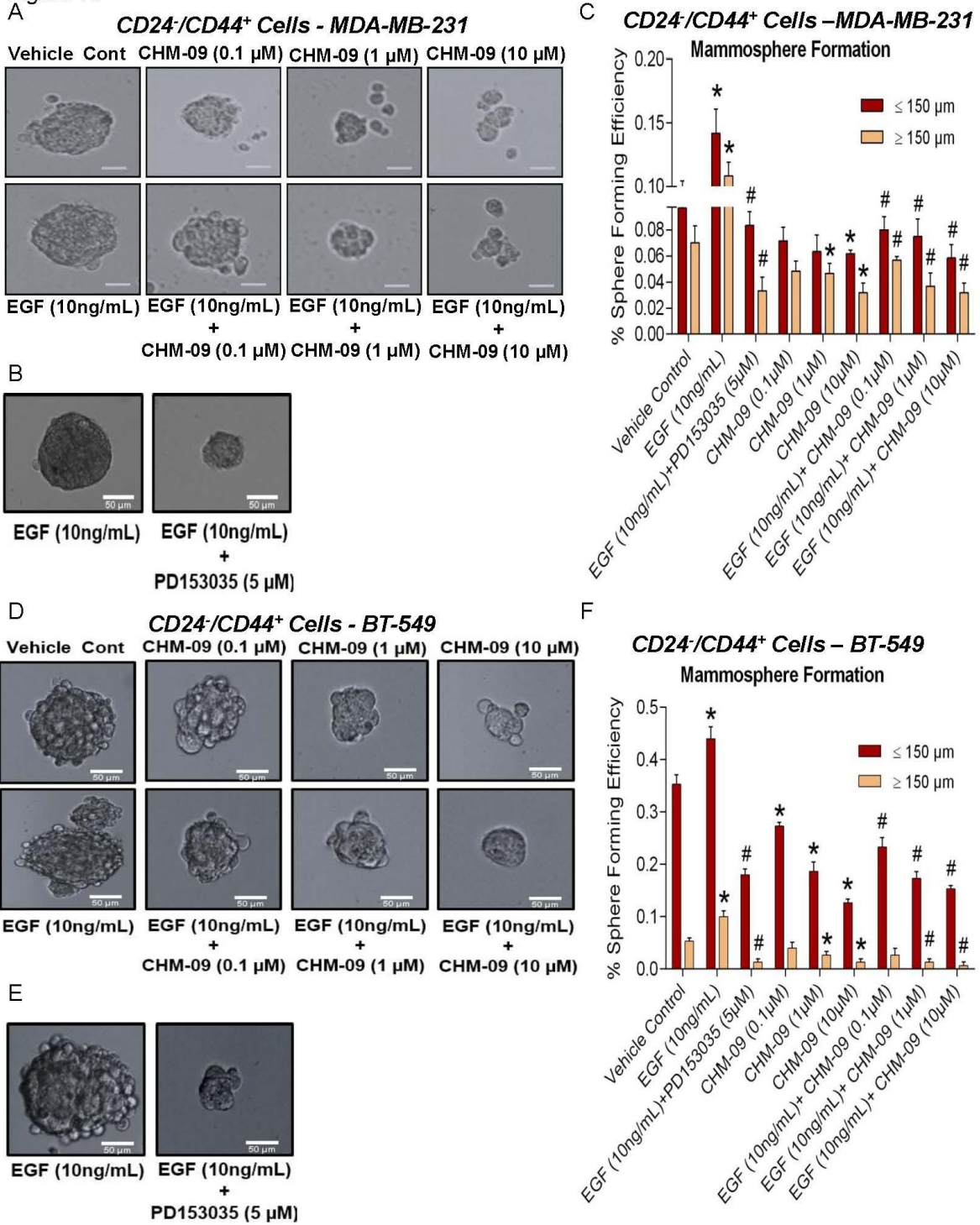


Figure 10. EGFR inhibition abrogated CSCs mammospheres forming efficiencies: Breast CSCs sorted from TNBCs –*MDA-MB-231* when subjected to (A) an increasing concentration of CHM-09 (5 μ M) in presence or absence of EGF (10 ng/mL) or (B) PD153035 (5 μ M) in presence or absence EGF (10 ng/mL) depicted a dose-dependent decrease in EGF-induced mammosphere formation (n=4). (C) Representative photomicrographs of mammospheres were quantified using image J software as described in the methods. Similar decrease in mammospheres formation efficiency was also observed in *BT-549* cells treated with (D) CHM-09 or (E) PD153035 in presence of EGF (10 ng/mL) as (F) quantified from representative photomicrographs (n=4). Scale bar: 50 μ m. Data are the mean \pm SEM from experiments repeated four times, p <0.05 (*t*-test) as compared to *vehicle control and #EGF-treated group.

Figure 11

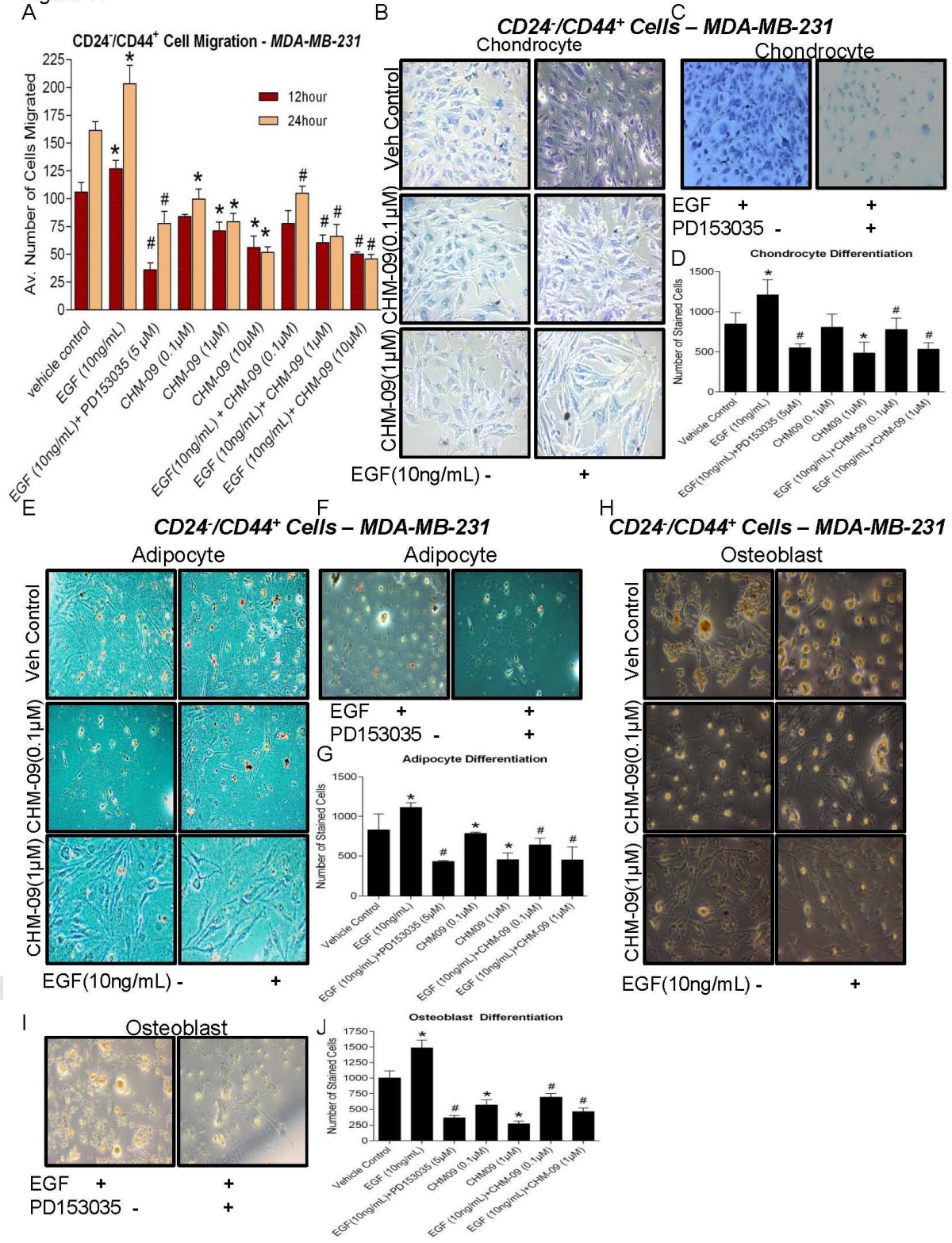


Figure 11. EGFR inhibition perturbs the migratory potential as well as tri-lineage differentiation ability in breast CSCs: (A) A time- and dose-dependent increase in EGF-induced migration of breast CSCs was significantly inhibited by EGFR blockers, CHM-09 and PD153035 (n=4). EGF-induced collagen deposition was significantly reduced in presence of (B) CHM-09 and (C) EGFR inhibitor, PD153035 and (D) quantification of representative photomicrographs as depicted in chondrocyte differentiation assay (n=6). Similarly, EGF treatment leads to an accumulation of oil O droplets that were decreased in presence of (E) CHM-09 (F) PD153035 and (G) representative image quantification as observed in adipocyte differentiation assay (n=6). Also, EGF-induced mineral deposits were significantly blocked by EGFR inhibition using (H) CHM-09 (I) PD-153035 and (J) photomicrographs quantification revealed in an osteoblast differentiation assay (n=6). Quantification of photomicrographs was performed using NIH Image J software. Data are representative of more than three independent experiments. p <0.05 as compared to *vehicle control and #EGF-treated group.

Figure 12

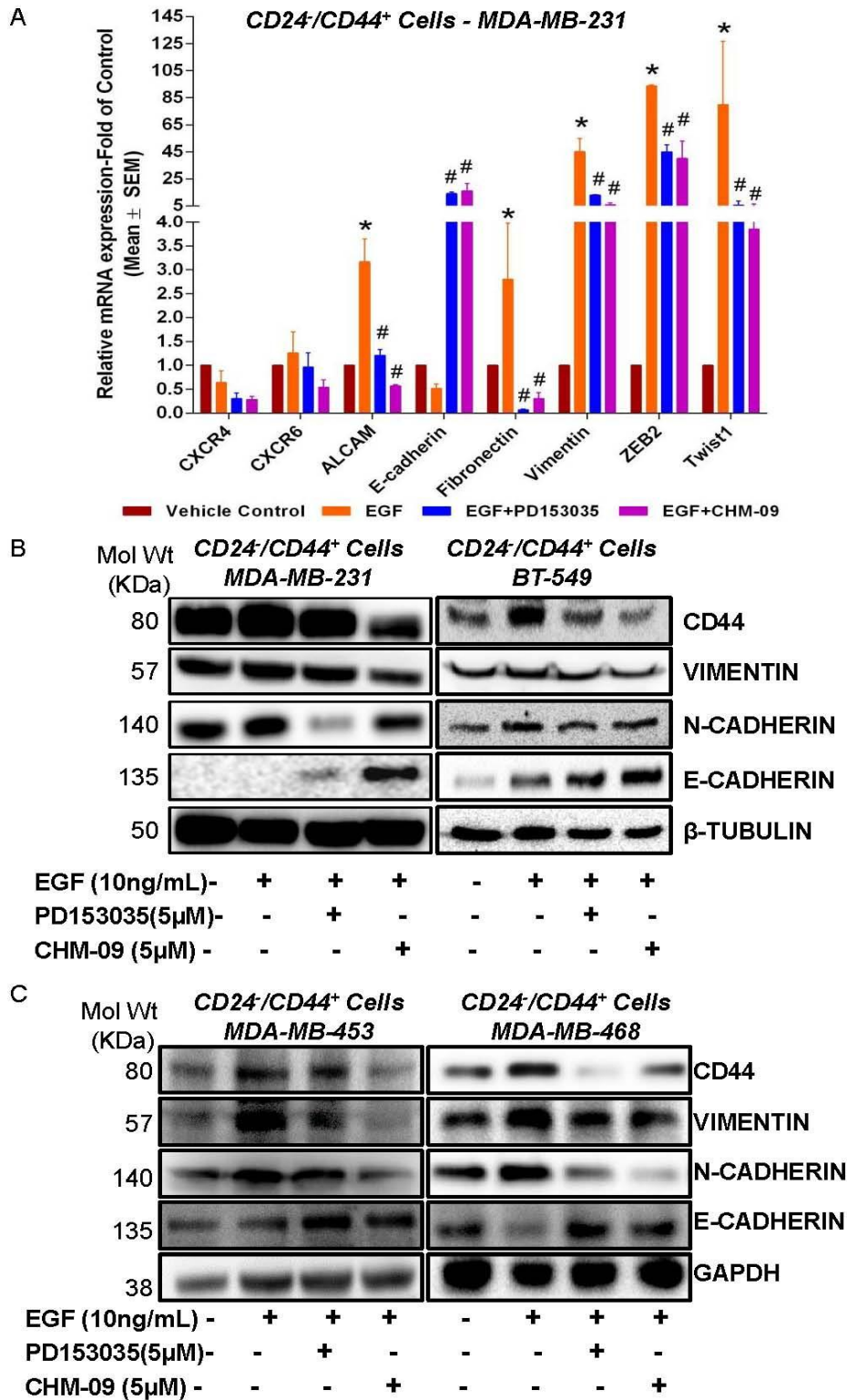
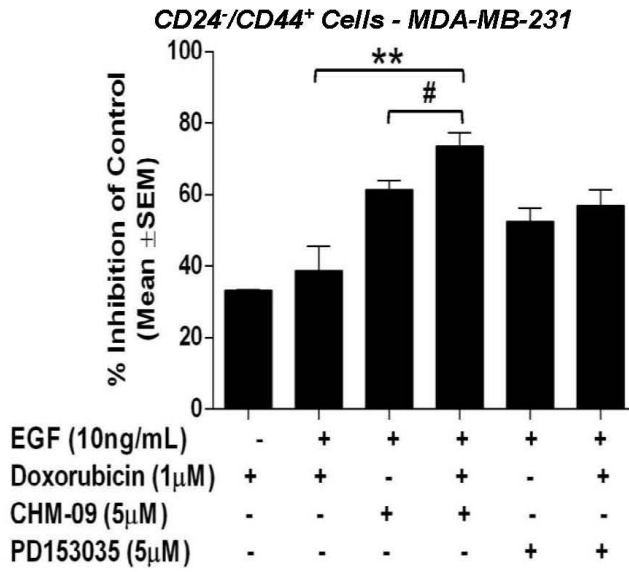


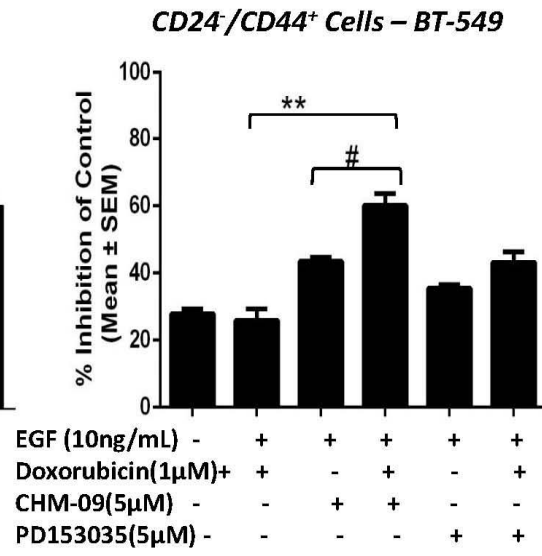
Figure 12. EGFR inhibition induces MET in breast CSCs: (A) A significant reversal of EGF-induced epithelial and mesenchymal gene expression in CSCs in presence of EGFR inhibition using CHM-09 and PD153035 (n=3). Immunoblot analysis in CD24⁻/CD44⁺-breast CSC sorted from (B) *MDA-MB-231* (left panel) and *BT-549* (right panel) as well as (C) *MDA-MB-453* (left panel) and *MDA-MB-468* (right panel) depicting decreased mesenchymal markers – vimentin, N-cadherin and CD44 and increased epithelial marker –E-cadherin in breast CSCs treated with CHM-09 or PD153035. Data are representative of three independent experiments. p <0.05 as compared to *vehicle control and #EGF-treated group.

Figure 13

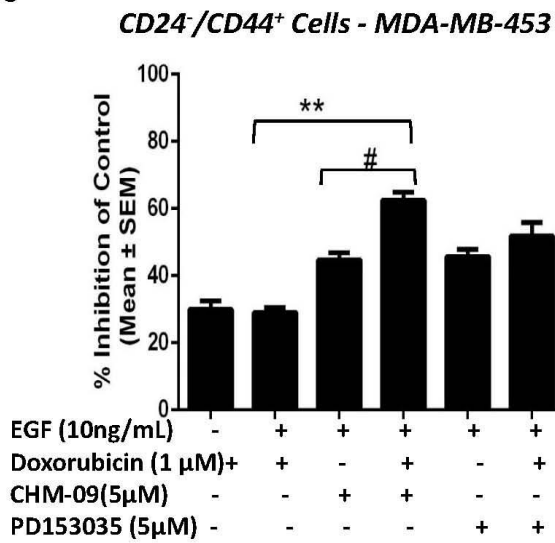
A



B



C



D

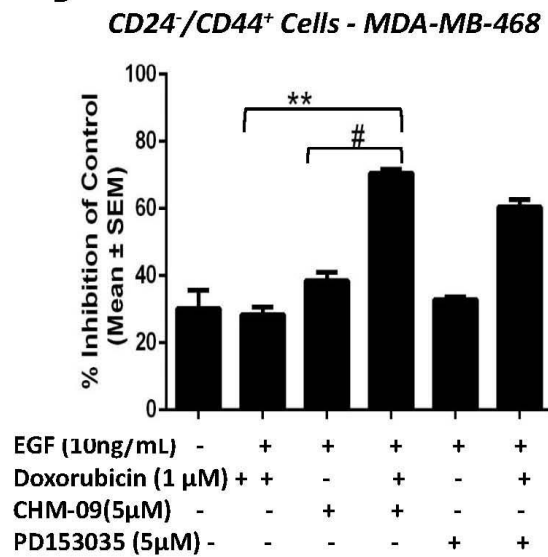


Figure 13. EGFR inhibition increases the responsiveness of breast CSCs to chemotherapeutics: Significant increase in the inhibition of breast CSCs proliferation was observed when simultaneously treated with EGFR blockers and anticancer drug, doxorubicin as compared to alone (n=6) in CSCs sorted from a panel of TNBC cell lines (A) *MDA-MB-231*, (B) *BT-549*, (C) *MDA-MB-453* and (D) *MDA-MB-468*. Data are the mean \pm SEM of three independent experiments, $p < 0.01$ (*t*-test) as compared to **control and #EGF-treated group.